5-2020

The Determination of Phosphorylation of Nato3 by PKA

Miranda M. Regenold
Grand Valley State University

The Determination of Phosphorylation of Nato3 by PKA

Miranda M. Regenold

A Thesis Submitted to the Graduate Faculty of

GRAND VALLEY STATE UNIVERSITY

In

Partial Fulfillment of the Requirements

For the Degree of

Master of Science in Biomedical Sciences

Department of Biomedical Sciences

May 2020

Abstract

One of the leading regulators of neuronal cell differentiation in the CNS is the family of basic helix–loop–helix (bHLH) transcription factors. One of these proteins, Nato3, is associated with the formation of dopaminergic neurons. Transcription factors can be regulated by kinase activity, and in order to detect the associated change of phosphorylation of Nato3, we have generated Nato3 with specific epitope tags that allow for the detection and isolation of the Nato3 protein. Through subcloning techniques and a successful transformation of the Nato3 gene with the sequences of the 3X-Flag epitope and the Myc epitope into the pcDNA3.0 vector, we were able to begin testing the phosphorylation status of Nato3. In particular, these epitopes attached to Nato3 allowed us to better detect the phosphorylation status and migration patterns in SDS-PAGE gels. We were able to see significant mobility shifts on the gels consistent with a phosphorylation event. This type of phosphorylation of the Nato3 protein will allow us to continue forward to determine the specific residue within Nato3 that is phosphorylated. Understanding the post-translational modification of Nato3 may help lead to better understanding of dopamine neurogenesis.

TABLE OF CONTENTS

LIST OF CHAPTERS

CHAPTER

LIST OF FIGURES

FIGURE

LIST OF TABLES

TABLE

CHAPTER I

INTRODUCTION

Parkinson's Disease: Impact and Overview

Parkinson's Disease (PD) is the second most prevalent neurodegenerative disease, after Alzheimer's disease, and affects at least 1 million Americans and 4-6 million people worldwide (Van Den Eeden, 2003). Research has shown that patients with PD have a five-fold higher chance of needing nursing home assistance compared to their non-PD counterparts, leading to an overall 4.8 times increase in economic burden (Vossius et al., 2009). During the progression of PD dopamine neurons die within the midbrain, specifically the nigrostriatal dopaminergic system which leads to debilitating motor impairments and many non-motor symptoms. Some of the physical motor symptoms include tremor, loss of stability, decreased gait, slower movements, and muscle rigidity (Kalia & Lang, 2015; Sveinbjornsdottir, 2016). The motor symptoms associated with PD are most easily recognized. What may not as easily be observed are the non-motor symptoms which include depression and anxiety, sleep disturbances, hallucinations, and many suffer from cognitive problems such as mild cognitive impairment or dementia (Sveinbjornsdottir, 2016).

Current Hypothesis of Pathogenesis: Braak stages of neurodegeneration

According to the Braak Staging hypothesis, the initial stage where neuronal death is observed is in the medulla and brainstem area. The death of DA neurons then proceeds into the locus coeruleus and dorsal nucleus in stage two. In stages, three and four (pre-symptomatic and symptomatic stages, respectively) the loss of dopamine neurons progress to the substantia nigra pars compacta (SNpc) and ventral tegmental area (VTA) midbrain regions, for stage three specifically, and meso-cortex in stage four. Finally, in stages five and six it spreads to the entire brain (Braak et al., 2003). The SNpc and VTA in the midbrain contain the large majority of the dopamine-containing cells. When the neurons within the SNpc die, dopamine neurons are no longer able to send their signals from the SNpc to the striatum. The amount of cell death is correlated with the severity of the disease (Ma et al., 2010). Normally, proper signaling between the SNpc and the striatum leads to proper motor control which allows smooth, purposeful movement as well as controls cognition and emotional behavior (Nunes et al., 2003). However, with the loss of dopamine signaling due to dopamine cell death causes abnormal nerve firing patterns within the brain that causes impaired movement (Omodei et al., 2008).

Cellular mechanisms of pathology: alpha-synuclein

Some of the leading research into the causes of PD has been with the protein alpha-synuclein and the formation of Lewy bodies. A primary marker associated with PD

is the presence of Lewy bodies that are aggregated from the protein alpha-synuclein present within the DA neurons themselves. It is thought that these elements could lead to neurodegeneration associated with PD (Braak et al., 2003). Alpha-synuclein makes up 1-2% of all the proteins within the central nervous system. Although alpha-synuclein function is unknown, there is evidence for a broad spectrum of functions including: the regulation of synaptic transmission and calcium transport, mitochondrial function, protein phosphorylation and regulating dopamine release (Ellis et al., 2005). Alpha-synuclein primarily destroys the presynaptic portion or terminal of a neuron suggesting that it plays a role in the transmission of neurotransmitters, such as dopamine.

One primary mechanism of pathogenesis that is currently being investigated is the misfolding of Alpha-synuclein which can oligomerize into beta-pleated sheets. This misfolded form of alpha-synuclein tends to be more stable than its original secondary structure making it very difficult to reverse. The stability of the beta-pleated sheets exposes hydrophobic regions, which has been assumed to be the reason why the misfolded alpha-synuclein can aggregate. When these proteins aggregate together, they form plaques leading to a dysregulation of dopamine release among other the symptoms associated with PD (Benskey et al., 2016). The release of DA, controlled by the firing rate of the neurons within the substantia nigra pars compacta is a key factor associated with maintaining proper levels of DA within the midbrain. This activity of the smaller midbrain region has effects on broad areas that it projects to the striatum, where more than 90% of the DA neurons in the brain ultimately synapse (Smith et al., 1994).

Cellular mechanisms of pathogenesis: mitochondrial dysfunction/oxidative stress

A significant indicator of PD seen in autopsied brain tissue is the presence of reactive oxygen species that arises from mitochondrial dysfunction (Dawson & Dawson, 2003). This dysfunction is due to mitochondrial complex I impairment which is considered to be the rate-limiting step in the overall reaction of the electron transport chain. The activity of complex I in the mitochondria is the initial step in the reaction and when inhibited leads to increases in oxidative stress, inflammation, and energy failure. These conditions can lead to increased aggregation of alpha-synuclein (Dauer & Przedborski, 2003; Dawson & Dawson, 2003; Schapira, 2008).

Interestingly, there are factors that have been shown to be neuroprotective against this type of stress. Research indicates that factors such as the engrailed-1 (EN-1) protein, is associated with protecting embryonic midbrain DA neurons against the toxic effects that can occur with mitochondrial complex-1 dysfunction as well as increase the overall mitochondrial complex 1 activity in synaptoneurosomes that is associated with mature adult neurons (Alvarez-Fischer et al., 2011)**.** Likewise, the Lmx1 genes Lmx1a and Lmx1b have been shown to be important in the regulation of mitochondrial function and the formation and survival of adult midbrain dopaminergic neurons (Doucet-Beaupré et al., 2016). Nato3, the protein that is the subject of our investigation, can elevate the expression of Lmx1b (Peterson et al., 2019), and unpublished data in our lab indicate that a modified form of Nato3 can elevate En1 broadly in CNS progenitor cells.

Therapeutic Interventions: levodopa

There are no pharmaceutical treatments to treat alpha-synuclein aggregation or Lewy bodies. Levodopa (L-DOPA) is the most commonly prescribed drug to treat PD. Administering patients DA directly does not treat the symptoms of PD because DA cannot cross the brain-blood barrier and is rapidly degraded. Instead, a precursor to DA, L-DOPA, is used for treatment of motor symptoms (LeWitt, 2015). L-DOPA, once in the periphery, can cross the blood-brain barrier and then can be converted into DA in the brain via the enzyme dopa decarboxylase (Hyland & Clayton, 1992). Carbidopa (trade names Sinemet and Pharmacopa) is also prescribed with L-DOPA because it is a periphery dopa decarboxylase inhibitor since L-DOPA can be converted into DA in both the periphery and brain, so administration of carbidopa with L-DOPA, allows L-DOPA to reach the brain and act on dopamine neurons (LeWitt, 2015). DA receptor agonists (such as apomorphine) can be used as a pharmaceutical treatment as well and can help with some of the motor symptoms associated with PD, however, these medications lose their efficacy over the course of the disease (Morizane et al., 2008). These medications only treat the motor symptoms and not necessarily the cause of PD. For the many individuals taking the medications there are still non-motor side effects that are not being treated, therefore neuropsychiatric disorders can then develop.

Therapeutic interventions: cell replacement therapy

The key concept behind cell replacement therapy application to PD patients is to restore the neurons that were once lost during the progression of the disease and create new fully functional DA neurons.

Early studies found that transplanted dopaminergic neuroblasts into the human PD striatum (the projection region of the midbrain DA neurons) showed moderate recovery of the disease and gave hope for future potential patients. However, the results were variable from patient to patient (Parmar et al., 2019) including the presentation of graft induced dyskinesias . Post-hoc analysis indicated that multiple factors, including the stage of disease the patient received the transplanted cells was a key factor in the positive impact of the treatment: patients with a shorter history of the disease showed stronger positive response to transplantation. Although many clinical trials have been underway, including a coordinated global effort with human induced pluripotent stem cells (iPSC), human embryonic stem cells (hESC) and fetal ventral midbrain cells (vMB), the primary endpoints of these trials are still just being reached. Of these efforts, human fetal tissue poses a large ethical concern and a limited source of tissue, making it less promising than stem cells as a potential treatment. Human eESCs can be differentiated into DA neurons, which has begun testing for safety in clinical trials (Palmer et al., 2019; Parmar et al., 2019). Another large factor associated with stem cell research is induced pluripotent stem cells (iPSCs) and it seems to have the same differentiation potential as ESCs, and can potentially generate new and fully functional DA neurons for transplantation into a PD patient (Parmar et al., 2019). These studies have progressed more quickly than hESC

studies and the first tests with human iPSC were transplanted into the patient's striatum in Japan in 2018 and we are waiting to hear the results (Parmar et al., 2020). Another promising study is Ma et al. (2010). This study tested advanced stage PD patients that were then treated with F-fluorodopa fetal dopamine graph transplants injected into the striatum. Because of the difficulty of getting to the SNpc, the striatum was used because it is where the DA neuron projection from the SNpc terminates. This treatment allowed for increased motor improvements in these patients and some of the clinical symptoms were alleviated. This showed that increased levels of DA is key to recovery.

Genesis of dopamine neurons and the role of bHLH factor Nato3

A region in the midbrain of the CNS that is known as the floor plate (FP) region gives rise to dopaminergic neurons derived from progenitor cells that are affected in PD (Ang, 2006). Nato3 (also known as N-Twist or Ferd31) is a basic Helix-Loop-Helix (bHLH) transcription factor has shown to be a key regulator of DA progenitor cell development. It is needed for proper neural development and the determination of the FP cell type, and has been shown to be necessary for DA neurogenesis (Ono et al., 2010). Specifically, previous studies involving knockout mouse models with the germline deletion of the Nato3 gene showed a decrease in the number of DA neurons by 50% (Ono et al., 2010). This study, in addition to gain of function studies conducted by this lab demonstrate that Nato3 is important in the regulation of gene expression of Lmx1a, Nurr1, and En1 (Andersson et al., 2006; Niu et al., 2018; Nouri & Awatramani, 2017). En1, Lmx1a and Lmx1b are expressed with Nato3 in floor plate cells and is specific to the floor plate region

of the mesencephalon located in the midbrain (Andersson et al., 2006; Ono et al., 2010). The expression of these key factors in floor plate and DA neuron progenitors is shown in Figure 1.

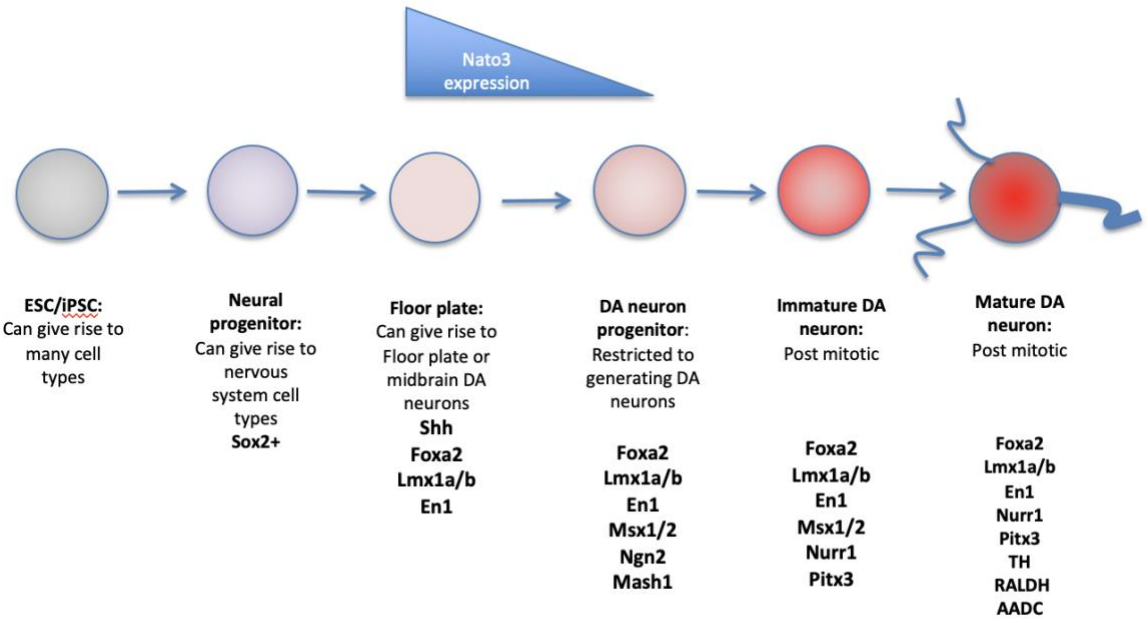

Figure 1. Progression of differentiation of stem cells into mature DA neurons and the expression of key dopaminergic factors.

Key factors such as Shh, Foxa2, Lmx1a, Lmx1b and En1 are co-expressed early in development with Nato3 gene. Nato3 has been shown to regulate the expression of some of these genes, although the mechanism is not understood.

Mechanism of action of Nato3: insights from other Basic-Helix-Loop-Helix (bHLH) Proteins

Helix-Loop-Helix (HLH) proteins are a family of proteins associated with transcriptional regulation for developmental processes including neuronal development (Massari & Murre, 2000). A subtype of HLH is the basic-Helix-Loop-Helix (bHLH), giving it a zipper effect as it binds around the DNA with the lysine and arginine amino acids. Some HLHs use an E-box site that coordinates certain gene transcription. The E-box interacts with the bHLH and they interact with the DNA to affect transcription. After dimerization, bHLH transcription factors bind E-box motifs with the consensus sequence, with the central two nucleotides, as well as surrounding nucleotides, providing specificity of binding (Bertrand et al., 2002).

One of the leading regulators of neuronal cell differentiation in the nervous system is the family of basic helix–loop–helix (bHLH) transcription factors (Bertrand et al., 2002; Parras et al., 2002). Within the central nervous system (CNS), Ascl1 (Mash1) is one of the key regulators of neurogenesis by dimerizing with its binding partner E47 and recruiting transcriptional activators to the promoters of important neuronal genes like tyrosine hydroxylase (Raposo et al., 2015). Interestingly, the action of Ascl1 on tyrosine hydroxylase promoter is regulated by a phosphorylation event at S152 by a protein kinase CK2 (Viñals et al., 2004).

Another example of posttranslational modification of bHLH is the bHLH Olig2 and the regulation of CNS stem cell differentiation into glia and neurons (Miller & Gauthier, 2007). During CNS development, some neuronal precursor cells are converted into

astrocytes and oligodendrocyte precursors that differentiate into myelin precursor cells. One of the key proteins associated with the switch from progenitors giving rise to oligodendrocytes instead of motor neurons is the transcription factor Olig2.

Interestingly, phosphorylation of Olig2 at S147 by the kinase enzyme cAMP dependent protein kinase (aka. PKA) is necessary for the oligodendrocyte precursors formation. In order for a phosphorylation event to occur the enzyme protein kinase covalently binds a phosphate group to the amino acid. An esterification reaction occurs when a phosphate group reacts with the hydroxyl (-OH) group of a serine, threonine, or tyrosine amino acid. In the Miller & Gauthier (2007) study, investigators used a Myc epitope-tag form of Olig2 and analyzed the phosphorylation status of the protein using a 2D polyacrylamide gel electrophoresis (PAGE) and western blot (WB) transfer. This and mass spectroscopy analysis revealed a phosphorylation event at a Serine 147 by PKA and another kinase known as protein kinase C (PKC). This phosphorylation motif, including the serine is conserved throughout most bHLHs (Li et al., 2011; Viñals et al., 2004). Li et al., (2011) also demonstrated that mutations of the PKA phosphorylation sites on Olig2 introduced into the mouse Olig2 gene disrupted the ability of the mice to generate oligodendrocyte precursors.

Our experiment

Similar to Ascl1 and Olig2 phosphorylation of Nato3 might be an important factor in the regulation of DA neurons, based upon our unpublished lab data. The mutation of Serine at position 140 to the negatively charged aspartate (S140D) is described as

phosphomimetic because the negative charge introduced at the 140 position can mimic phosphorylation. Early studies in the lab targeted mutagenesis of this site because s this S140 mutation is homologous to the mutations attempted at the homologous Ser in Olig2 and Mash1. This phosphomimetic mutant of Nato3 showed a functional change by driving increased expression of dopamine neuron related genes (Shh, Foxa2, Lmx1b, Nurr1) when expressed in neural progenitors in the developing chick embryo. However, it has not been shown that Nato3 is the substrate of a kinase. In the present study, we generated stable, epitope-tagged Nato3 constructs to determine expression of phosphorylation of Nato3 by PKA (cAMP-dependent protein kinase). This epitope-tagged form of Nato3 will be able to be used as a building block for future studies to conduct mass spectroscopy to identify specific sites of phosphorylation as well as to visualize Nato3 location within in vivo conditions. Here we generated epitope constructs and monitored if Nato3 phosphorylation by PKA could be detected by a mobility shift using a both a SDS-PAGE as well as a modified SDS-PAGE approach known as Phos-tag SDS-PAGE.

CHAPTER II

METHODS FOR EXPERIMENTATION

Transformation

In order to generate plasmids that contain the Nato3 with flag epitope we thawed frozen DH5a bacteria on ice. Then in chilled culture tubes, we added 5 µL of DNA per 50 µL of DH5a. Flicked the tubes several times to mix them and then returned them to ice for 30 minutes. We heat shocked the cell mixture for 45-60 seconds at 42°C. Then put the tubes back on ice for 5 minutes. We added 900 µL of SOC media to each tube and incubated at 37°C for 60 minutes with shaking. After shaking, we plated 100 µL of undiluted media onto agar plates with ampicillin. The other 800 µL was then spun down into a pellet and about 600 µL of the supernatant was disposed of, and the pellet was resuspended into the leftover supernatant media before 100 µL was plated onto agar plates with ampicillin. The plates were then incubated overnight or for 12-14 hours.

Mini Prepreperation

Using the transformed bacteria grown, a colony was picked and put in 3mL of LB ampicillin in round bottom 15mL falcon tubes that sat overnight shaking in 37°C. 600 µL were then put into 1.5 mL eppendorf tubes that then were spun down for 1 minute. Continue as per Zymo mini preparation protocol.

Agarose Gel

Using 1g Agarose and 100mL of 1x TAE we heated the mixture at 50% power in a microwave for 10 minutes, while stirring in between to ensure the solution did not boil over. We cooled the mixture in water until it was cool enough to touch then added 10 µL of gel safe and poured it into gel mold. We took it out, loaded the gel and ran them at 120V.

Isolation of DNA from agarose gel

We added 3 volumes of Binding Solution II to one volume of gel slice (100 mg = 100 µL). Incubated it at 50°C for 10 minutes with occasional vortexing or until the gel slice had been completely dissolved. DNA was isolated from the mixture per Genscript manufactures instructions.

Restriction Digest

In order to release the insert of the associated epitopes from IDT, we added a restriction enzyme buffer (Cut Smart), 5U of Not1HF and EcoR1HF into an eppendorf tube. We then incubated the mixture for 2 hours at 37°C before running on a 1% TAE agarose gel. For the isolation of the linearized pcDNA3.0 by Not1 and EcoRI, a calf intestinal phosphatase (CIP) was added to prevent re-ligation. The linearized vector and inserts were isolated from the 1% TAE agarose gel containing 1:10,000 GelSafe reagent and then the gel was visualized under long wavelength UV light.

Ligation of insert and vector

We added 10 ng/μL (100 ng) of the EcoRI and NotI cut pcDNA3.0 vector, 5 ng/μL (50 ng is ideal) of cut insert, 1uL of 10mM ATP, 1 μL of 10x ligation buffer, and 0.67 μL DNA ligase. We incubate the mixture at room temperature for 15 minutes. We then incubated the mixture for 30 min at 37°C. After incubation, we placed the reaction in a 70°C water bath for 15 minutes to deactivate the DNA ligase and then continued with transformation protocol to grow cells containing the new vector with the desired insert, or stored at -20°C until transforming.

Cell culture

We thawed a frozen HEK cell plug, and added drop wise in a 10 cm tissue culture dish with 10 mL of Dulbecco's Modified Eagle's Medium with 10% Fetal Bovine serum (DMEM-10) media. We passed cells every 3-5 days depending upon cell growth confluency (want 80%-90% confluent). We made sure all liquid media that was used was warm to the touch prior to use. When passing cells we discarded media carefully. Next, we added 4 mL of phosphate buffer saline (PBS) and then discarded. After, we added 4 mL of ethylenediamine tetraacetic acid (EDTA), then discarded. By tapping the petri dish we were able to disrupt cell clumps and then would add 5-7 mL of DMEM-10 media to cells and pipette up and down to mix the cells. Then we added 2-3 mL of cell culture mixed media to 7-8 mL of fresh DMEM-10 once again into a 10 cm plate.

Immunocytochemistry

We grew the cells to 80% confluency. For fixation, we incubated the coverslips in freshly prepared 4% paraformaldehyde for the 1xFlag Nato3 construct, and for the Nato3 detection experiment in ice cold acetone for 10 minutes. then in PBS at room temperature for 10 minutes and then washed the coverslips in PBS for 5 minutes. In order to reduce the background fluorescence for blocking, we blocked the coverslips in 5% normal serum for 1 hour at room temperature. We then incubated the coverslips with the primary antibody in a 1:200 dilution in 1% BSA (Nato3 Goat Polyclonal to Human NATO3;

LSBioworks, Cat# LS-C305867) for 1 hour at room temperature. Then we washed the coverslips gently in PBS three times for 5 minutes each. We then incubate the coverslips in the secondary antibody (Nato3 Donkey Anti-Goat igG H&L (Alexa Fluor 555); abcam) in a 1:10,000 dilution in 5% BSA for 1 hour at room temperature in a dark environment. Then we washed the coverslips gently in PBS for three times 5 minutes each.

Transfection

In a 1.5 mL eppendorf tube we added 312.5 µL of DMEM and X µL of DNA (determined based on concentration of sample) and then vortexed the mixture together. Experimental conditions included transfection of epitope-tagged Nato3 in the pcDNA 3.0 vector alone or in combination with C-alpha and/or PKI on the CMV.Neo vector backbone. We then added 12.5 µL of P3000 reagent and set aside. In a separate Eppendorf tube, we combine 312.5 µL of DMEM and 9.3 µL of Lipofectamine reagent and vortexed that mixture. We combine the two mixtures and let them sit at room temperature for 10-15 minutes. Then add drop wise into 6 well plates.

Induction of phosphorylation

We monitored the effect of the phosphorylation status of Nato3 in the presence of PKA during each of the phases of the differentiation process. Cells were cultured in 6 well plates to approximately 80 percent confluency. Thirty-six hours after transfection, HEK

cells were washed twice with phosphate-free DMEM (Invitrogen). The cells were then washed twice with ice-cold PBS and harvested. Proteins were separated by SDS-PAGE gel electrophoresis, and visualized using western blot analysis.

Harvesting and isolation of crude extract

We harvested cells from a six well plate or 10 cm plate in 500 µL of RIPA buffer. NP40 lysis buffer (50 mM HEPES-KOH, pH 7.5, 150 mM KCl, 2 mM $MgCl_2$, 2% v/v NP40, 0.5 mM DTT, 1 × complete EDTA-free protease inhibitor cocktail (Sigma). We then centrifuged at 1,500 rpm for 10 min at 4°C and removed the supernatant. We then vortex the tubes briefly and proceed to sonication with 30 sec ON/30 sec OFF with a total sonication time of 5-10 cycles at a temperature of 4°C . We stopped sonication after 5 cycles, briefly vortexed and then visually checked the samples. We then transferred the supernatant to a new tube and centrifuged the samples at 14,000 rpm for 15 min at 4°C to remove any remaining insoluble material. Finally, we aliquoted 10 ul for quantification with a protein assay and stored protein extracts at -80°C. Finally we added 1 volume of 2x Laemmli buffer to the rest of the solution (about 200 µL) if not doing TCA for a phos-tag gel.

Protein concentration assay

The standard protocol was performed in a 250 µL 96 well microplate assay with a linear range of these assays for BSA is 125–1,000 µg/ml. For the 2 mg/ml BSA we followed the following standard curve.

5 ml Standard Assay

Tube #	Standard Volume (µl)	Source of Standard	Diluent Volume (µl)	Final [Protein] (µg/ml)
1	300	2 mg/ml stock	0	2,000
2	375	2 mg/ml stock	125	1,500
3	325	2 mg/ml stock	325	1,000
4	175	Tube 2	175	750
5	325	Tube 3	325	500
6	325	Tube 5	325	250
7	325	Tube 6	325	125
8 (blank)	–	–	325	0

We pipetted each standard and unknown sample solution into separate clean microplate wells, added the 1x dye reagent to each well and mixed the samples. We incubated the samples at room temperature for at least 5 min, measured the absorbance of the standards and unknown samples using a spectrophotometer at 595 nm. We then used a linear regression of the absorbance of the BSA standard to convert the absorbance of samples into known protein concentration.

TCA precipitation

From harvested cells we used the TCA precipitation to clean up the protein before running a Phos-tag gel. We added 2 µL of 2.5% DOC to each protein sample, vortexed and incubated it at 37°C for 10 minutes. Next, we added 200 µL of 20% TCA, vortexed and

incubated on ice for 5 minutes. We then centrifuge at max speed, 4°C for 10 minutes and then removed the supernatant. Next we added 500 µL of ice-cold acetone, vortexed and repeated the centrifuge at max speed, 4°C for 10 minutes before removing the supernatant, adding 500 µL of cold acetone, and vortexing again. We again centrifuged at max speed again for 10 minutes at 4°C. Next, we aspirated the acetone and added 2x laemmli buffer (about 100 µL) and 100 µL RIPA, resuspend, vortexed and then sonicated.

SDS-PAGE/Phos-Tag

We used enough cell lysate samples for equal amounts of total protein into 0.5ml microfuge tubes. We added a 2X SDS-PAGE laemmli buffer mix, and a range of 10-50 µg of total protein were used. The samples were heated up to 95-100°C for 20 minutes. Then we loaded the total volume of the sample onto the acrylamide gel, along with a pre-stained molecular weight marker. A stir bar was used along with a stir plate, and the gel was run at 95V until the samples were stacked at the interface between the stacking and separating gel. After, the gel was run at up to 150V making sure it did not go above 385 mA, and while running the gel we prepared a PVDF membrane (Cat # 1620177; BioRad, Herceles, CA) by soaking it in methanol for a few seconds, washing in H2O, and equilibrating it in Transfer Buffer for 10 minutes. The gel was removed for the SDS-PAGE and we set up the transfer cassettes submerged in the transfer buffer. Once completion occurred, we soaked the gel in a blocking solution (3% gelatin solution in TBS) overnight or for 12-14 hours to allow for staining.

Western Transfer

Using the whole protein extract of the crude form of Nato3 we fractionated the protein by SDS-PAGE and transferred it onto a polyvinylidene difluoride membrane using a transfer apparatus according to the manufacturer's protocols (Bio-Rad). When we ran a phos-tag gel, we soaked the gel in EDTA for 10 minutes prior to adding it to the rest of the material for the transfer. We soaked the PVDF paper in 100% methanol briefly and rinsed it in Western Transfer Buffer (25 mM Tris, 192 mM glycine, pH 8.3, 20% methanol). We also soaked 2 pieces of filter paper and whatman paper in the transfer buffer. On a transfer apparatus, we took one piece of filter paper and laid it on the bottom of the apparatus with extra buffer present, and rolled over the top of the paper with a small roller to ensure no bubbles were present. Next, we layered the PVDF paper (rolled to get bubbles out), then the gel (rolled to get bubbles out), and then the second piece of filter paper (rolled to get bubbles out). After ensuring the apparatus was on tightly we ran it at 20V, with no more than 385 mA for 1 to 2 hours.

Staining

We made the staining buffer (3% gelatin in TBS (10 mM Tris, pH 8.0, 150 mM NaCl)) fresh each time. We also made the primary antibody (1:1000 of antibody buffer of horseradish peroxidase-conjugated anti-mouse or anti-rabbit antibodies and M2 antibody) and put in 4°C, and made the secondary antibody (1:3000 of antibody buffer of horseradish peroxidase-conjugated anti-mouse or anti-rabbit antibodies and AP

conjugate) then put in 4°C. Then we blocked the filter paper in the staining buffer for 30 minutes at room temperature on a shaker. Next, we washed once with TTBS solution (10 mM Tris, pH 8.0, 150 mM NaCl, 0.5% Tween 20) for 5 minutes at room temperature on a shaker, Added cold primary antibody mixture and then let sit for 30 minutes at room temperature on a shaker. We then washed three times with TBST, each for 5 minutes, added the cold secondary antibody mixture and let it sit for 30 minutes at room temperature on a shaker. Next we washed it twice with TBST for 10 minutes, and then in TBS for 5 minutes to remove the tween 20 in the TBST mixture. Finally, we supplied freshly made 1x color developing buffer from the BIORAD color developing buffer kit and let it sit at room temperature. The antibodies were targeted against the epitope-tag on Nato3.

CHAPTER III

Results

Transcription factors can be regulated by kinase activity, and in order to detect the associated change of phosphorylation of our protein, we will look for a shift in the mobility of the Nato3 protein in the SDS-PAGE under phosphorylation conditions. The only commercially available Nato3 antibody (LSBioworks; Cat# LS-C305867) that has been demonstrated to detect Nato3 protein functions effectively with light fixation in immunohistochemistry and immunocytochemistry (Mansour et al., n.d.), and is not a functional agent in western blot or more stringent fixation conditions such as paraformaldehyde.

A common strategy to circumvent this issue is to add a sequence of amino acids to the protein that is known to be an effective epitope to a specific and effective antibody, such as FLAG (Asp-Tyr-Lys-Xaa-Xaa-Asp) or Myc sequence (Glu-Gln-Lys-Leu-Ile-Ser-Glu-Glu-Asp-Leu). Therefore, we used an epitope tagged form of Nato3 to allow us to detect the protein in assays such as mobility shift in SDS-PAGE conditions. We expressed a single Flag sequence attached to the amino terminus of the mouse Nato3 open reading frame that had been generated in this lab previously.

This epitope form of Nato3 (called 1xFlag Nato3) was expressed in HEK 293T cells to determine successful expression of 1x Flag Nato3 construct using the bicistronic GFP vector (pCIG) as the expression vector (Figure 2). We were able to successfully transfect

cells as indicated by GFP expression (data not shown) and sought to detect Flag epitope on Nato3 using paraformaldehyde fixation, as outlined in Figure 2 part a. Using a 4% PFA (paraformaldehyde) fixation (10 minutes at room temperature) and staining solution allowed our Flag to be more accessible. Using fluorescence microscopy techniques we were unable to detect our Flag constructs (Figure 2 part b). This, in addition to an inability to detect the expression of 1xFlag Nato3 in western blot (data not shown) led to the conclusion that the 1xFlag epitope on Nato3 was not functional.

To ensure that Nato3 portion of Flag could be detected, we used the lighter fixation process that permits Nato3 antibody to recognize the Nato3 protein outlined in Figure 3a. These images show that the Nato3 protein can be detected amongst cells expressing the construct. (Figure 3b). DAPI counterstaining allows the visualization of nuclei, identifying the total number of cells in the micrograph. Figure 2 part b panel 3 shows the overlay of cell nuclei and those cells expressing the Nato3 protein.

Based upon our results with fluorescence microscopy, we determined that our 1x Flag Nato3 construct was not detectable. In order to determine why our construct was not visibly detectable, we then submitted the constructs for DNA sequencing using primers that flanked the open reading frame of the Nato3 gene. We identified an error with the nucleotide sequence (Figure 4). After reviewing the sequence and realizing the missing nucleotides in the sequence is most likely leading to it's undetectability with our Nato3 protein. Thus the next phase of my thesis work included designing and testing new epitope-tagged constructs for Nato3.

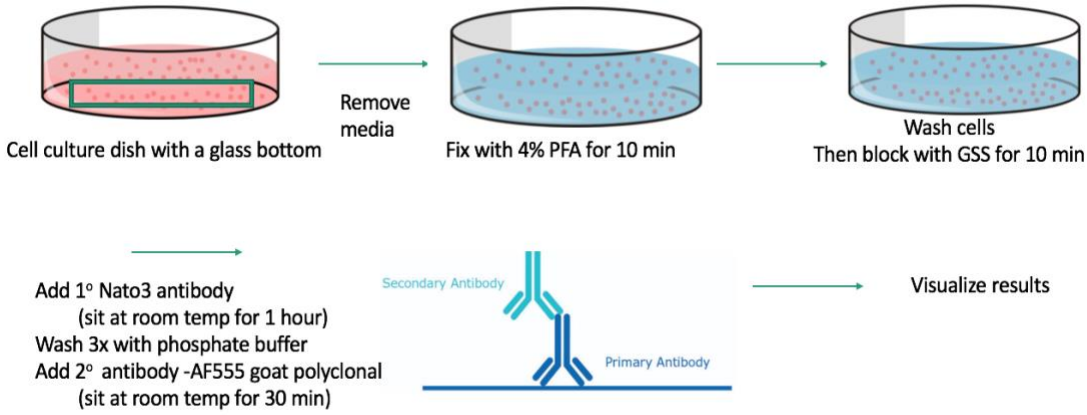

A.

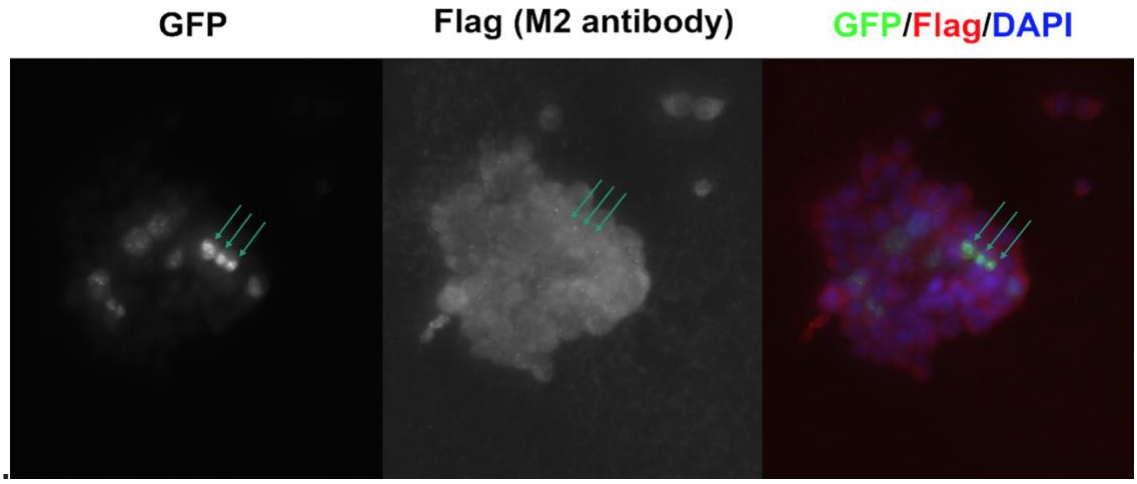

B.

Figure 2:1xFlag Nato3 construct cannot be detected by Nato3 antibody in PFA fixation by Immunocytochemistry

Part A. The methodology process used for fluorescence microscopy using 4% PFA fixation in cells that have been transfected with the bicistronic GFP and 1xFlag Nato3 vector. The expression of GFP indicates cells that should co-express the Nato3 protein.

Part B. The first panel (left) shows the presence of GFP in cells that identify cells that should also express Nato3 presence and detectability. The middle panel does not show our epitope-tagged constructs that would be used to show the presence of and detectability of our constructs. This led to the realization that there was an error associated with the constructs. The right panel shows the results with the nuclear counterstain DAPI.

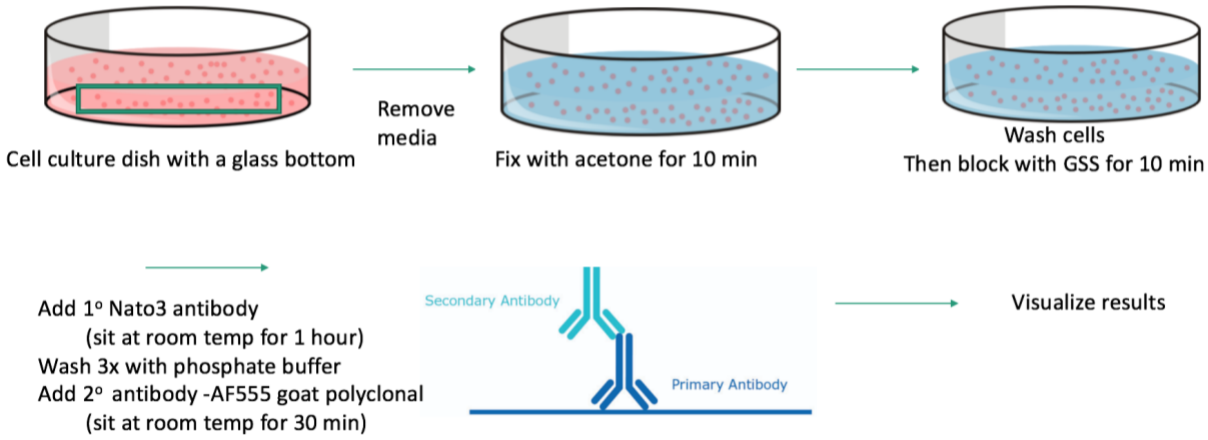

A.

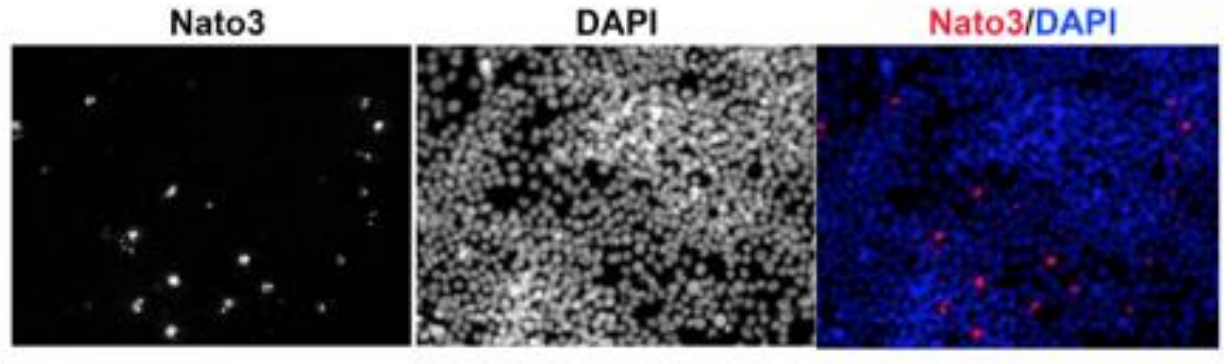

B.

Figure 3: Nato3 can be detected by Nato3 antibody in acetone fixation by Immunocytochemistry

Part A. The methodology used for detection of the Nato3 protein using acetone fixation.

Part B. The first panel (left) shows the presence and detectability of the Nato3 protein in cells. The middle panel shows the nuclear counterstain DAPI to show all the present cells. The last panel (right) shows the overlay of DAPI stain and the detectable Nato3 protein.

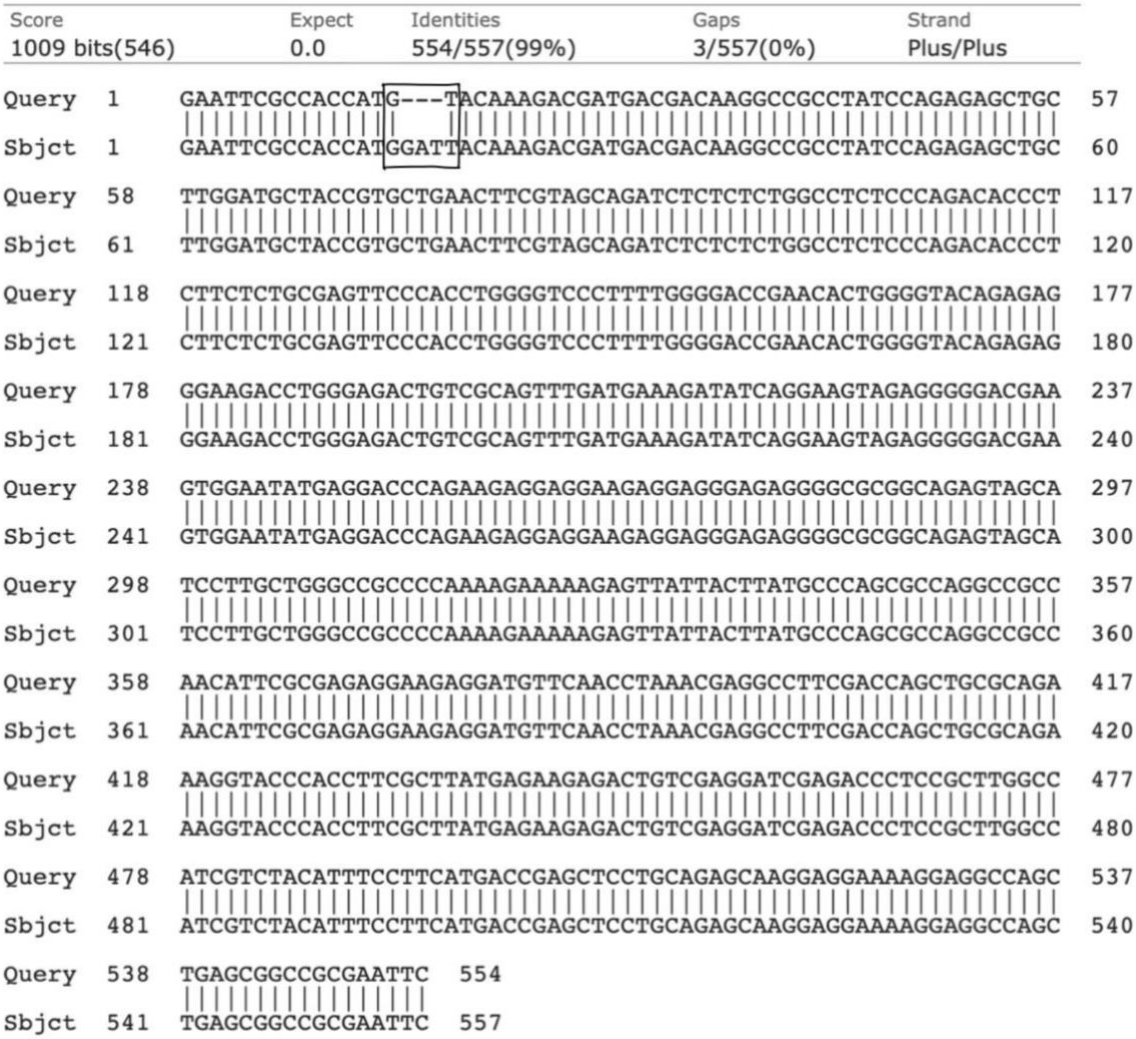

Figure 4: DNA sequence of the 1xFlag sequence error and correct sequence

The query sequence (top sequence) is the 1xFlag Nato3 sequence used for the fluorescence microscopy expressed in Figures 1 and 2. The sbjct sequence (bottom sequence) is the correct template DNA sequence for 1xFlag that includes the full sequence of amino acids in the Flag epitope (Met-Asp-Tyr-Lys-Asp-Asp-Asp-Asp-Lys). The box indicates the 3 missing DNA nucleotides in the 1xFlag Nato3 construct that encoded the first amino acid “Asp” of the epitope. That explained why there was no detectability of the 1x-Flag version of Nato3.

Generation of new epitope-tagged Nato3 constructs

It is critical that the epitope tag does not disrupt protein stability while being successfully expressed. Previous literature demonstrated that a Myc epitope tag of the amino-terminus (N-terminus) the bHLH proteins Neurogenin (Perez et al., 1999) and Ascl1(Mash1) (Viñals et al., 2004) did not affect the stability (or function as measured in the reports) of the proteins. In the case of Nato3, we wanted to test if the location of the epitope tag affected stability, so we generated N-terminus and carboxy-terminus (C-terminus) affinity tags.

Since our protein is expressed while in mammalian cells, we decided to use tags that have been successful in mammalian cells. One such flag is the triplet version (3xFlag) of the first construct we attempted (1xFlag Nato3). The nucleotide sequence of the 3xFlag encodes 23 amino acid sequences that contain the Asp-Tyr-Lys-Xaa-Xaa-Asp motif repeated three times. This improves the detection of the protein by the ANTI-FLAG® M2 antibody. Figure 5 part a illustrates the generation of the amino acid sequence of the epitope-tagged protein, N-terminus 3xFlag Nato3.

The Myc epitope tag is another tag that can be easily detected, has been linked to bHLH proteins before and expresses well in mammalian cells. The Myc tag is a protein tag that comes from the c-Myc gene that can be added to a protein in the form of a tag through recombinant DNA technology. This generated another form of Nato3 that we could test for stability. If successful, this construct could be useful in future biochemical experiments that require a different epitope than Flag epitope.

We submitted the open reading frame (ORF) of the epitope-tagged forms of Nato3 to IDT (Integrated DNA technologies, Coalvilled IA) for construction into a vector with flanking EcoRI sites and a 3' Not I site. This IDT vector was transformed into bacteria, grown on LB selection media and prepared subcloning by excision with Not1 and EcoRI. Through subcloning sequencing, we were able to do a successful transformation of the Nato3 gene with the sequence of the epitope for the N-terminal 3X flag and the C-terminal Myc flag into a pcDNA3.0 vector. The pcDNA3.0 vector is a mammalian expression vector with a CMV promoter. The multiple cloning site of this vector allowed us to take advantage of a process known as directional cloning allowing us to cut the vector at both EcoR1 and Not1 sites. This ensured that the tagged-protein stayed in its correct linear orientation when inserted as well as when cut during a restriction digest (Figure 5 part b).

(N-term3xFlag WT Nato3 mouse)

GAATTCGCCACCATGGACTACAAAGACCATGACGGTGATTATAAAGATCATGACATC
GATTACAAGGATGACGATGACAAGGCCGCCTATCCAGAGAGCTGCTTGGATGCTAC
CGTGCTGAACTTCGTAGCAGATCTCTCTCTGGCCTCTCCCAGACACCCTCTTCTCT
GCGAGTTCCCACCTGGGGTCCCTTTTGGGGACCGAACACTGGGGTACAGAGAGGG
AAGACCTGGGAGACTGTCGCAGTTTGATGAAAGATATCAGGAAGTAGAGGGGGAC
GAAGTGGAATATGAGGACCCAGAAGAGGAGGAAGAGGAGGGAGAGGGGCGCGGC
AGAGTAGCATCCTTGCTGGGCCGCCCCAAAAGAAAAAGAGTTATTACTTATGCCCA
GCGCCAGGCCGCCAACATTCGCGAGAGGAAGAGGATGTTCAACCTAAACGAGGCC
TTCGACCAGCTGCGCAGAAAGGTACCCACCTTCGCTTATGAGAAGAGACTGTCGAG
GATCGAGACCCTCCGCTTGGCCATCGTCTACATTTCCTTCATGACCGAGCTCCTGC
AGAGCAAGGAGGAAAAGGAGGCCAGCTGAGCGGCCGCGAATTC

Flag sequence
GAC TAC AAA GAC CAT GAC GGT GAT TAT AAA GAT CAT GAC ATC GAT
TAC AAG GAT GAC GAT GAC AAG

A.

B.

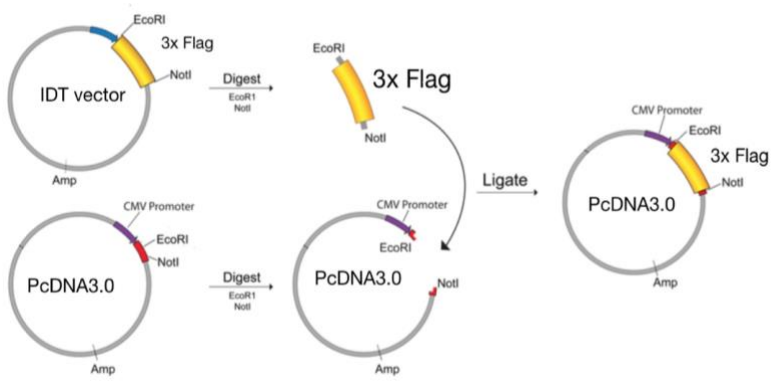

Figure 5: Generating Epitope Constructs

Part A. Illustrates the DNA sequence of the N-terminus 3x Flag (dark blue) with Nato3 (no associated color) with flanking EcoRI sites (aqua) and 3' Not I site (magenta).

Part B. Demonstration of the subcloning strategy from the vector of the 3X flag Nato3 (yellow insert) constructed from the manufacturer IDT (labeled as IDT vector) into our mammalian expression vector pcDNA3.0.

Preparation and ligation of pcDNA3.0 expression vector and Nato3 epitope inserts

To prepare the expression vector for the new epitope-tagged forms of Nato3, we had to linearize pcDNA3.0 with restriction enzymes EcoR1 and Not1. By cutting with two distinct restriction enzymes we ensure that an insert with complementary ends is ligated in a single orientation, a strategy described as directional cloning (Sambrook & Russell, 2006). We performed agarose gel electrophoresis saturated with Gelsafe DNA stain to isolate pcDNA3.0 and the constructed inserts and observed (Figure 6a), pcDNA3.0 migrating at the correct size of 5446 bp. We were able to successfully excise the pcDNA3.0 from the gel and treated it with phosphatase to remove terminal phosphates and prevent religation of the vector with itself. Using NotI and EcoRI we also excised the 3xFlag and Myc epitope and identified bands at 573 bp and 558 bp, respectively and successful separation from the parent IDT vector (at 2.7 kb) (Figure 6b and 6c, respectively). To prepare the epitope-tagged form of Nato3 into the parent vector the bands were excised under low wavelength ultraviolet light allowing the visualization and isolation of the DNA from the agarose gel. We then used the isolated DNA for the ligation of the epitope-tagged form of Nato3 (3xFlag Nato3 and Myc-Nato3) with the pcDNA3.0 vector. The bands with the white boxes around them in Figures 5a, 5b, and 5c, show the exact bands that we excised from the gel directly.

The EcoRI and NotI linearized the pcDNA3.0 vector and cut the epitope-tagged Nato3 insert and then were ligated in the presence of DNA ligase. Given that we had the ability to do directional cloning if we had a successful ligation, we were confident that the

insert would be added with the sense strand in the 5' to 3' direction in accordance with the vector (see Figure 5B). In order to isolate plasmids that contain the epitope-tagged Nato3 lighted into pcDNA3.0 in the ligation mixture we performed a transformation into DH5 alpha competent cells and plated on LB plates with ampicillin as the selection agent.

Identifying successfully generated epitope-tagged Nato3 pcDNA3.0 clones

We chose five colonies from LB-AMP plates for each ligation transformation and grew small scale cultures (3ml), isolated plasmid DNA and performed a restriction digest with the DNA. If our directional cloning strategy was successful, we would see two bands: one for the pcDNA3.0 vector that we released the insert from (at 5.4 kb), and a second band for our insert. For N-3xFlag and C-Myc epitope-tagged Nato3 inserts, we would see bands at 573bp and 558 bp. If we did not see an insert then the most likely alternative is that we would see a band at 5.4 kb, corresponding to the empty pcDNA 3.0 vector.

We fragmented the restriction digest of the 10 different clones on a 1% agarose gel. We observed a successful restriction digest of both the epitope-tagged insert and the pcDNA3.0 vector and found a successful N-3xFlag (Figure 7A) and two successful C-Myc inserts (Figure 7B) separated from the vector. The PcDNA3.0 vector is 5.4 kb and can be seen above the 3kb rung of the DNA ladder (GeneRuler 100 bp Plus DNA Ladder; ThermoFischer) and the inserts are running just above the bright 500 bp fragment of the DNA ladder). In some of the lanes (lane 3 in N-3xFlag Figure 6A and lanes 1 and 5 in C-Myc Figure 7B) we also see bands migrating slightly above and below the linearized vector, consistent with incomplete cutting of the circular plasmid DNA yielding two species

of uncut plasmid known as nicked and supercoiled (Balagurumoorthy et al., 2008). This allowed us to determine that we had successfully been able to ligate the pcDNA3.0 vector and insert for both N-3xFlag and C-Myc epitope-tagged Nato3 inserts. We then grew large scale 50 ml bacterial cultures and isolated epitope-tagged Nato3 pcDNA3.0 from each of these cultures to express in mammalian cells.

Successful expression of epitope-tagged Nato3 in mammalian cells

Epitope tagged Nato3 pcDNA3.0 constructs were transfected in human embryonic kidney (HEK) 293T cells and allowed to incubate for 24 hours prior to harvest. This allowed expression of the epitope-tagged Nato3 construct. During the transfection, pCIG GFP was co-transfected with the epitope-tagged Nato3 pcDNA3.0 constructs at a 1:10 mass ratio to be able to determine the efficiency of transfection by visualizing GFP+ cells. By adding a GFP expressing vector along with the pcDNA 3.0 vector that contained the Nato3 construct this allowed us to assume that if we saw GFP, then the other vector (pcDNA3.0) was transfected in the cells as well. Giving a rough estimate of transfection efficiency. Cells were then harvested, whole-cell extract isolated and protein concentration assayed. The whole-cell extract was then fractionated on a 4-20% gradient SDS polyacrylamide gel. The SDS-PAGE gel was then transferred to polyvinylidene fluoride (PVDF) membrane using the semi-dry western transfer method, blocked with a 1% gelatin solution and stained with antibodies directed against the 3xFlag or cMyc epitopes. Figure 8 shows the expression of the N-3xflag-Nato3 construct at 21 kDa. The

anti-FLAG® M2 antibody recognizes the FLAG® sequence (N-Asp-Tyr-Lys-Asp-Asp-Asp-Asp-Lys-C) at the N-terminus or C-terminus locations of proteins.

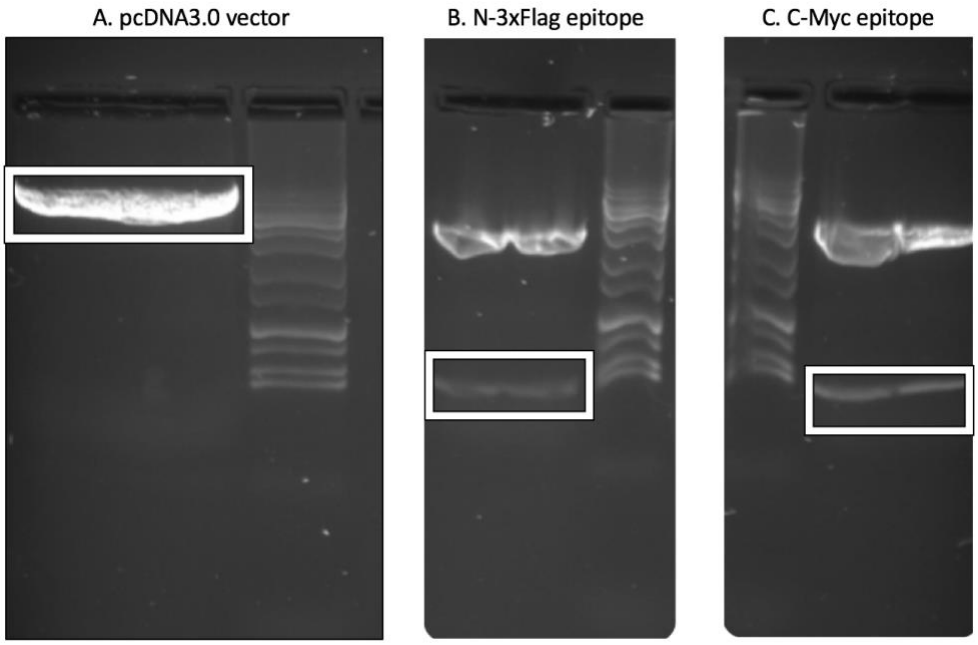

Figure 6: Visualization of DNA fragments to be excised and utilized for epitope-tagged Nato3 pcDNA3.0 vector construction

Part A. The 5.4 kb band on this 1% agarose gel corresponds to pcDNA3.0 linearized with Not and EcoRI that was excised (box) and used for ligation with the epitope-tagged Nato3 insert.

Part B. The DNA fragment that contained the epitope-tagged Nato3 insert (N-3xFlag) is shown in 5B (box) in the lower band (573 bp). The parent IDT vector is the upper band in figure 5B at the predicted size of 2.7 kb.

Part C. The DNA fragment that contained the epitope-tagged Nato3 insert (C-Myc) is shown in 5c (box) in the lower band (558 bp). The parent IDT vector is the upper band in figure 5c at the predicted size of 2.7 kb.

Displaying the successful separation with N-3xFlag and C-Myc from the parent vector. The C-3xFlag insert did not separate from the parent vector during this restriction digest.

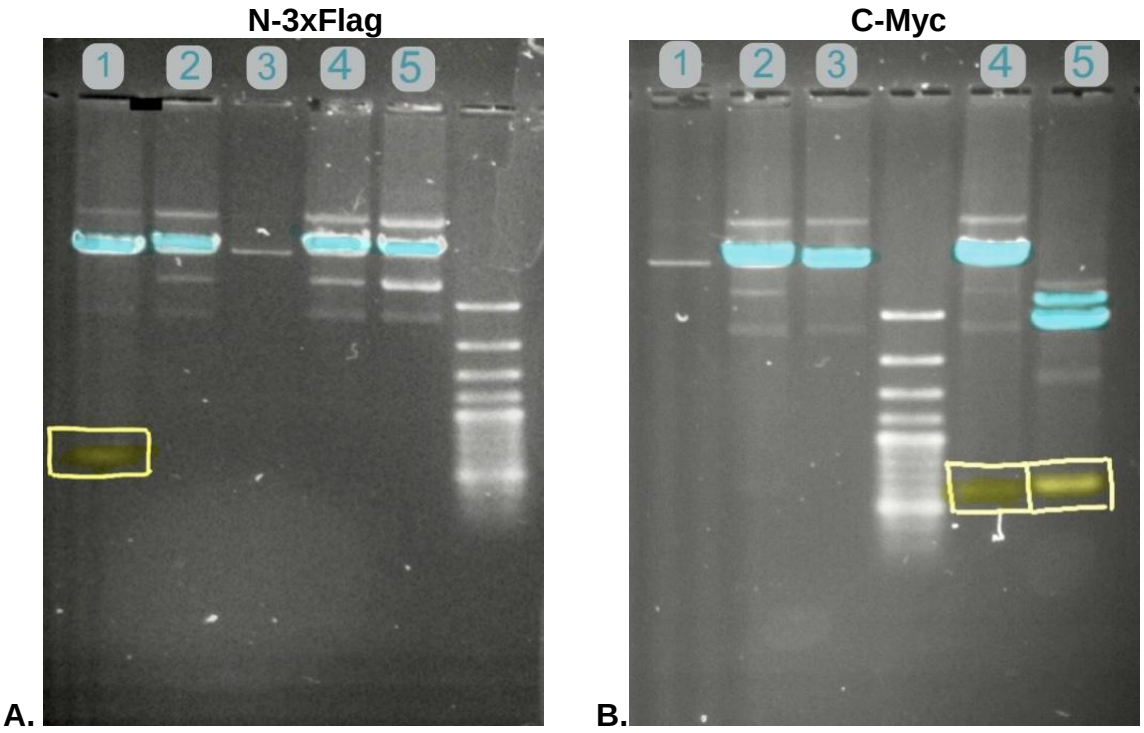

Figure 7: Restriction Digest of N-3xFlag and C-Myc from pcDNA3.0

Part A. Our data shows the successful restriction digest of the N-3xFlag in lane 1 (yellow box above) from pcDNA3.0 (highlighted in blue).

Part B. Our data shows the successful restriction digest of C-Myc in lanes 4 and 5 (yellow box above) from pcDNA3.0 (highlighted in blue).

Determination of expression and migration of epitope Nato3 construct under phosphorylation conditions

To better understand how 3xFlag epitope-tagged Nato3 functions in the presence of a kinase, we wanted to test the expression and migration in an SDS PAGE gel in the presence of a cell membrane analog 8CPT-cAMP that activates PKA that is endogenously expressed in the HEK 293T cells. As a negative control, we co-expressed a protein-based inhibitor of PKA. Initially, we anticipated a mobility shift to occur in the 8CPT-cAMP condition, however, that was not what was observed. Figure 9 shows how when our flagged-Nato3 protein was in the presence of PKI we see minimal protein expression. When comparing our epitope-tagged Nato3 alone to our epitope-tagged Nato3 in the presence of PKI and 8CPT-cAMP we see less expression, but not as low as in the PKI only condition. The darkest band with the highest intensity is the 8CPT-cAMP condition, suggesting that the epitope-tagged form of Nato3 is influenced in some way by proteins that lead to phosphorylation.

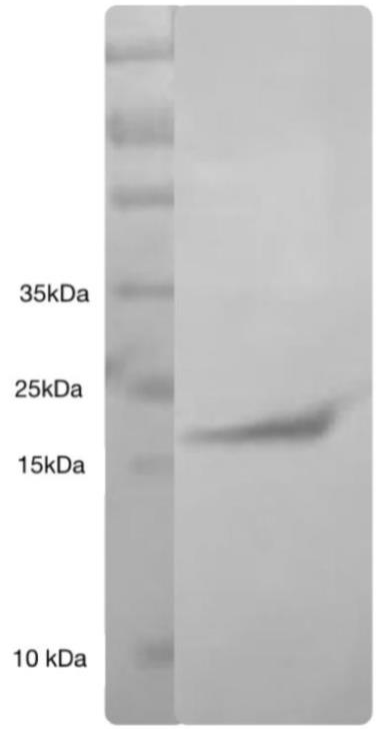

Figure 8: N-terminal 3x Flag-Nato3 can be stably expressed in HEK 293T cells.

HEK 293T cells were transfected with the N-terminal 3x Flag Nato3 construct and fractionated on a 4-20% gradient SDS-PAGE. The band with the predicted size of 21.2 kDa appears to the right of the molecular weight ladder between 15 and 25 kDa, indicating that the protein product is detectable and a stable product was generated.

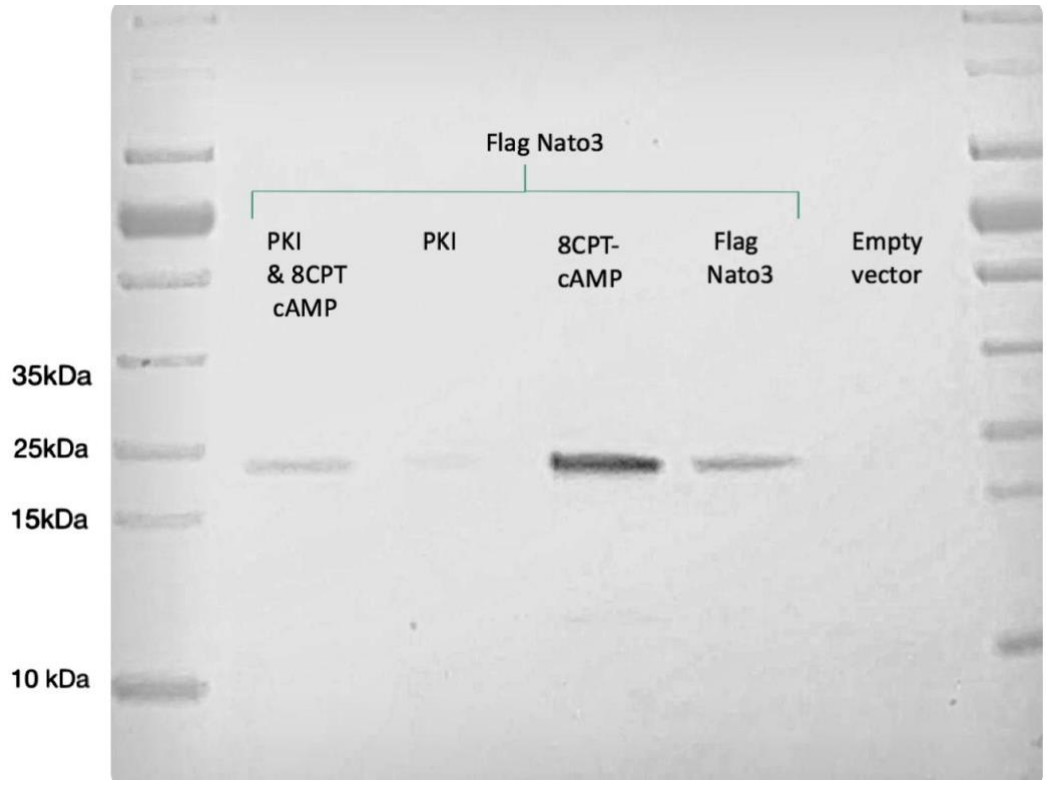

Figure 9: SDS-PAGE and Western Transfer of 3xFlag-Nato3 with PKI and cAMP 8CPT

We ran an SDS-Page gel and western transfer of our 3xFlag epitope-tagged Nato3 protein in the presence of a protein kinase inhibitor (PKI) and 8CPT-cAMP a cell membrane analog. When flag-Nato3 is in the presence of PKI, the expression level diminishes greatly, but a faint amount of expression can be detected. The expression levels of flag-Nato3 under both the PKI and 8CPT conditions (far left) show about the same level of expression as 3xFlag Nato3 alone. When 8CPT-cAMP is present 3xFlag Nato3 shows a very large amount of expression and the associated band is much darker than any other conditions. This indicates that there is an increase in protein expression levels.

Screening for a shift in mobility in epitope Nato3 constructs under phosphorylation conditions

It may be that the action of the cAMP analog for the four-hour incubation is not robust enough to promote the phosphorylation of epitope-tagged Nato3. Thus we tested if the constitutively active kinase of PKA is sufficient to cause an upward mobility shift in the newly generated epitope-tagged Nato3 constructs. Figure 8 shows that with co-expression of constitutively active PKA we find a greater protein expression level for both 3xFlag and Myc- tagged Nato3 in all conditions with PKA present. In both the 3xFlag and the Myc conditions we loaded volumes of 15uL and 5uL with a concentration of approximately 200ug/ml loaded into the gel (3mg and 1mg /well respectively). For both loading conditions (3mg and 1mg/well) t, we see greater overall expression levels for both conditions, however, relative to Myc tagged Nato3, the band intensity for 3xFlag is much greater in all the 3xFlag conditions (both with and with PKA). For the 3xFlag Nato3 with PKA conditions, we observed a slowly migrating band that appears around 30 kDa (star, Figure 10), in addition to the thicker bands visible at the expected migration of epitope-tagged Nato3 of 21 kDa. This upper band is consistent with a mobility shift associated with the phosphorylation of Nato3. This mobility shift is only detected in the Flag condition, not detected in Myc condition with the band residing around 21 kDa predicted value, although the slower migrating band in Myc condition may not be detected because of the weaker intensity of the signal. We also identified a lower band at 12 kDa, likely a degradation product of the Nato3 protein.

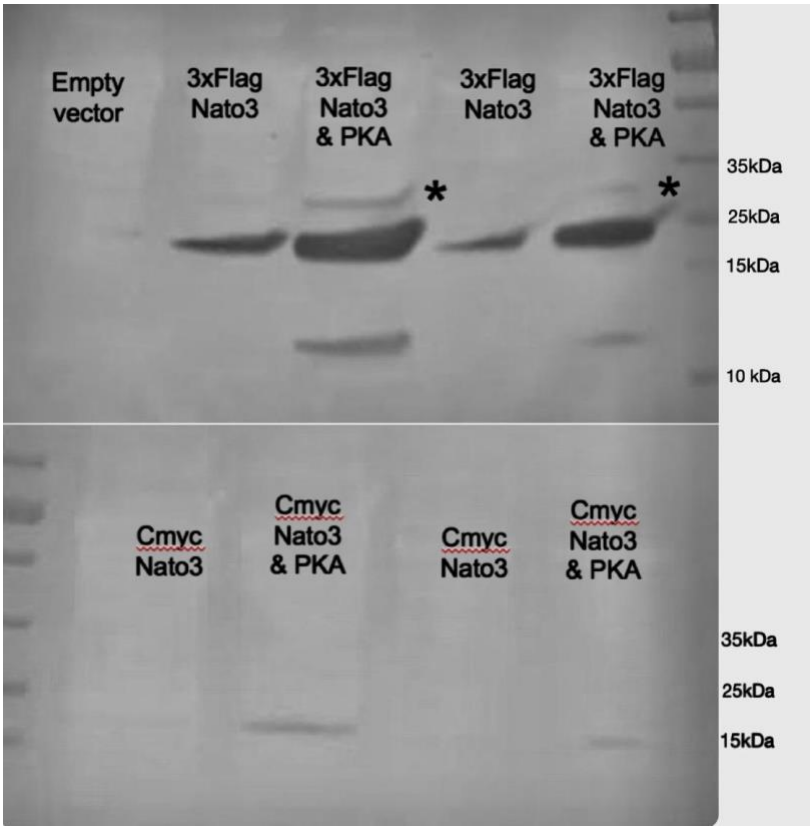

Figure 10: SDS-PAGE and Western Transfer of The Flag Constructs

We ran an SDS-Page Gel of an empty vector, N-3xFlag, N-3xFlag with PKA, (upper gel) C-Myc, and C-Myc with PKA (lower gel) in both 3mg/well and 1mg/well volumes, respectively. In both cases the protein product was detectable, indicating that a stable product was generated.

In both cases with N-3xFlag and PKA, expressed as the constitutively active catalytic subunit the results suggest that there is an increase in protein production/stability.

The upward shifted bands for both of the N-3xFlag with PKA conditions (starred) in the left image indicate that there may be a potential phosphorylation event happening as well.

Screening for a shift in mobility in 3xFlag-Nato3 construct with a Phos-tag gel

Due to the observed mobility shift in 3xFlag-Nato3 with PKA discussed previously, we wanted to conduct a similar experiment on an SDS-PAGE that is permeated with a chelating agent known as “Phos-tag” (Fujifilm). The Phos-tag chemical has preferential binding to a phosphorylated protein, so the Phos-tag chemical further slows the migration of the phosphorylated protein. Phosphorylation of the protein was determined by comparing the migration of the band for our epitope-tagged Nato3 by itself and when phosphorylated by PKA (Figure 11). We observed a single band for the epitope-tagged Nato3 alone condition similar to that seen with the SDS-PAGE condition in Figure 9. When the epitope-tagged Nato3 was in the presence of PKA we saw a very large mobility shift expressed as the smearing pattern as well as a much darker band indicating phosphorylation events occurring. We observe multiple bands in the mobility shift yielding a smearing pattern indicating that this could be due to phosphorylation at multiple sites.

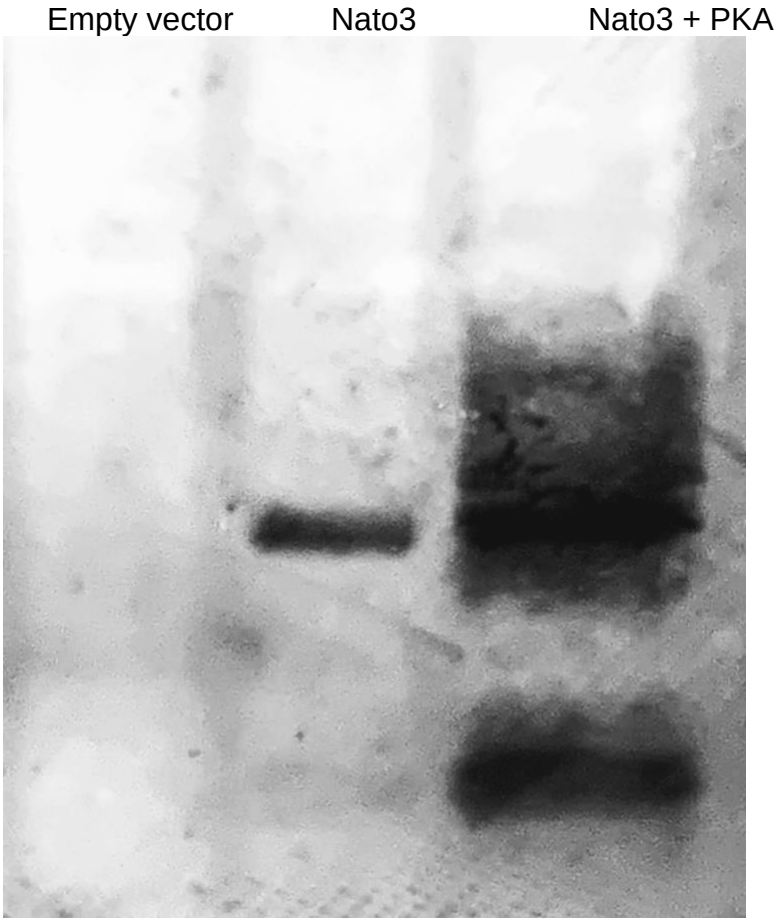

Figure 11: SDS-PAGE Phos-Tag gel and western transfer of 3xFlag-Nato3 construct

We ran an SDS-Page Phos-tag gel and western blot of 3xFlag-Nato3 with and without PKA. The Phos-Tag gel allowed us to visualize a different kind of mobility shift in the 3xFlag-Nato3 protein alone (left band) and when 3x-Flag Nato3 is in the presence of PKA (right band). This type of broadness in the band shift in the PKA condition is indicative of increased levels of phosphorylation of the protein.

CHAPTER IV

Discussion

Constructing new epitopes

After we had discovered that our previous tags contained a coding error (Figure 1 and Figure 3) we needed to construct new epitope-tagged Nato3 constructs. We had previously used a construct of 1xFlag, which likely would have worked if we had decided to fix the DNA sequence.however, we determined that the triplet version (3xFlag) of our initial 1xFlag was more likely to increase our detection of the tagged protein, due to the triple nucleotide repeat offering more epitopes to the anti-flag M2 antibody (Zhang et al., 2001).

We used the pre-generated nucleotide sequence of the 3xFlag is a synthetic peptide of 23 amino acid residue and the Asp-Tyr-Lys-Xaa-Xaa-Asp motif is repeated three times in the peptide. We also constructed another known epitope tag (myc epitope) that has been shown to be effective with other bHLHs such as Mash1 (Viñals et al., 2004) and Neurogenin (Perez et al., 1999). Prerez et al., (1999), expressed the Myc epitope tag at the amino terminus of Neurogenin 1 and 2. Viñals et al., (2004) expressed the Myc epitope tag in the Mash1 protein, and found increased stability of the protein with the expression.

We added our epitope-tags to both the N-terminus and C-terminus Nato3 for both 3x-Flag and Myc sequence conditions. These sequences were outsourced and made by

IDT and sent to us individually as they were synthesized, so we had initially received the N-3xFlag, C-3xFlag, and C-Myc epitopes. We received the C-3xFlag epitope towards the end of the overall project.

The N-3xFlag epitope-tagged Nato3 protein was much easier to detect in the SDS-PAGE gel compared to the C-Myc epitope-tagged Nato3 protein (Figure 8). We believe that one potential factor for this is that the N-3xFlag epitope tag is better detected in the blots due to the three separate epitope sequences associated with 3xFlag compared to the single epitope for Myc (Hernan et al., 2000; Zhang et al., 2001).

Another factor that may have led to the decrease in expression of the Myc sequence could be that there were not enough protease inhibitors included in the purification buffer (Konsoula, 2020). These protease inhibitors would ensure we had a more intact and non-degraded tagged protein. Therefore, the protein itself could have been degraded some, leading to the decrease in the efficiency. Another factor associated with the decrease in expression could be that the affinity of 3xFlag is greater than the affinity of Myc (Corp, n.d.), however, that is not something we can determine at this time without a proper Nato3 antibody to allow for this specific comparison (not an epitope tag antibody).

Nato3 acts as a substrate for PKA

Phosphorylation controls multiple signal transduction cascades associated with protein regulation. Proteins can have a phosphorylation-dependent electrophoretic mobility shift (PDEMS) in sodium dodecyl sulfate-polyacrylamide gel electrophoresis

(SDS-PAGE) (Lee et al., 2019). Under standard conditions, monomers of SDS bind to the hydrophobic regions of the protein, creating a mixture of alpha-helices that the SDS binds to and random coil regions that are naked of SDS (Shirahama et al., 1974). These “necklace and bead” structures tend to saturate at 1.4 g SDS/g protein for globular proteins (Reynolds & Tanford, 1970). Membrane bound proteins tend to run slightly differently from their predicted molecular weight due to the hydrophobic nature of the membrane associated regions altering the ratio of SDS: protein binding (Rath et al., 2009). Protein phosphorylation induces an electrophoretic mobility shift by inhibiting the binding of SDS chemicals to the peptide bonds of the proteins due to the charge-charge repulsion of the negative phosphate group and the positive sodium in the SDS mixture. This decrease in the ratio of bound SDS per protein results in the mobility shift.

Based upon our present data above, the epitope-tagged form of Nato3 suggests it is phosphorylated by PKA when tested using an SDS-PAGE gel. Figure 10 shows an 8kDa shift in mobility for the condition when N-3xFlag Nato3 is in the presence of PKA in the standard SDS-PAGE condition. This type of mobility shift is consistent with what is observed in phosphorylation-dependent SDS page mobility shift seen in other proteins. For example, Lee et al., (2019) observed an electrophoretic mobility shift in the phosphorylated form of Enzyme IIA when separated by SDS-PAGE using a 4–20% gradient polyacrylamide gel. Similarly, an approximately 5 kDa shift can be seen between the de-phosphorylated and phosphorylated form of vasodilator-stimulated phosphoprotein (VASP) which is a phosphorylation assay for platelet response to cilostazol and is used as a reliable measure of PKA activity within cells treated with PKA agonists.

To determine if there are species that are phosphorylated by PKA that may not be detected easily by SDS-PAGE we monitored protein mobility in SDS-PAGE that contained a chelating complex called "Phos-tag". In a Phos-tag gel there is a dinuclear metal complex (1,3bis[bis(pyridinyl-2-methyl)amino]propan-2-olato dizinc(II) complex) that acts as a phosphate-binding tagging molecule (“Phos-tag”) in an aqueous solution (Kinoshita et al., 2009). The Phos-tag molecule binds to a phosphate creating a phosphomonoester dianion. If there is a sufficient difference in the charged phosphate density then phosphorylated protein will have a slower migration and will be observed at a higher molecular weight on the gel in comparison to the non-phosphorylated protein (see Figure 12). In the Phos-tag SDS PAGE gel with 3x-Flag Nato3 under phosphorylation conditions (Figure 11) we observed multiple bands migrating more slowly than the predicted size of 21 kDa indicating that the gel is allowing us to see many different species being phosphorylated when Nato3 is in the presence of PKA. The smearing pattern may represent the aggregates that are more phosphorylated or phosphorylation at different sites giving many different bands. The 21 kDa band of the N-3xFlag Nato3 PKA condition that is at the same kDa size as the band in the N-3xFlag Nato3 alone condition. This likely represents the unphosphorylated form of the protein.

Another interesting observation is the difference in the expression of Myc and 3xFlag-tagged Nato3 protein in the PKA or cAMP analog condition. For both the SDS-PAGE and Phos-tag SDS-PAGE we observe a darker band whenever PKA or the membrane permeable agonist of PKA is present, in both the 3xFlag-Nato3 with PKA (see Figures 10 and 11), as well as a darker band present with Myc-Nato3 (see Figure 10). This effect of phosphorylation of bHLH stability has been shown before. Viñals et al., 2004

found that the Mash1/E47-dependent phosphorylation of serine 152 (homologous to Nato3 residue serine 140) seems to disrupt the protein conformation associated with proper degradation of Mash1. This means that the phosphorylation occurring in the PKA and 8CPT-cAMP condition may keep the protein in a more stable conformation and therefore allow more accumulation of the protein prior to its degradation. Indeed the mechanism of this effect in Ascl1 relies on the serine that is homologous to serine 140 in Nato3 (the proposed PKA phosphorylation site). In Ascl1 this effect is due to the dimerization occurring between the phosphate and serine residue which in a bHLH is located in a solvent-exposed loop between helices 1 and 2. In the model proposed by Vinals et al., (2004) this type of dimerization change would lead to the change in the overall net charge (from the negatively charged phosphate ion) leading to the increase in the heterodimer stability.

It is important to note that the effect of PKA and 8CPT-cAMP on Nato3 expression could be due to the promoter on the expression vector itself. Cytomegalovirus (CMV) promoter, found in our pcDNA3.0 vector, is commonly used in mammalian expression systems and possesses a CREB response element (CRE). PKA, either expressed or activated by 8-CPT-cAMP can phosphorylate endogenously expressed CREB, which is a transcription factor that can drive transcription through the CMV promoter like the one we used for epitope tagged Nato3 (Keller et al., 2007). Thus stability may not be affected but instead expression. To test this a PKA insensitive expression system could be utilized, or transient induction of PKA by short incubations of the 8CPT-cAMP analog (30 minutes) may allow sufficient time for phosphorylation without affecting expression, which usually needs a longer period of time to be seen.

As a way to show that phosphorylation is the cause for both the upper band seen in Figure 10 and the smearing pattern in Figure 11, phosphatase could be used. With the same transfected whole cell lysate material we could add phosphatase before running another gel. This would allow for the phosphates that bind to the epitope-tagged version of Nato3 to be cleaved and if phosphorylation caused the shift, then in this condition, there would be no upper band or smearing pattern occurring. This would lead to the conclusion that phosphorylation of Nato3 by PKA was what is observed in the gels and it would not be due to a difference in the level of protein expression.

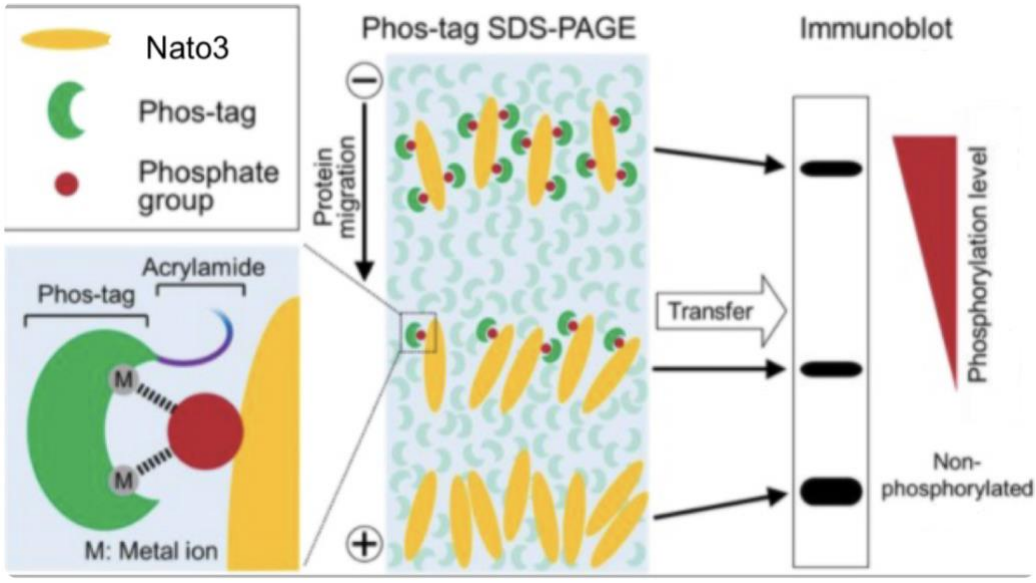

Figure 12: Diagram of Phos-tag immunoblot analysis

This schematic represents the action of the Phos-tag agent on the phosphate group on Nato3 through the metal ion, Zn^{2+}. The non-phosphorylated and phosphorylated forms of Nato3 are then separated by mobility through SDS-PAGE by the use of acrylamide conjugated with Phos-tag. Nato3 is then detected by the Anti-Flag epitope antibody. The upper band created by the mobility shift represents the phosphorylated protein that has retarded migration due to by the Phos-tag. Multiple phosphorylations of Nato3 could appear as different upward shift bands.Adapted from (Sato et al., 2017).

Protein degradation

We observed a 12kDa band in both the SDS-PAGE gel and the SDS-PAGE Phos-tag gel in the PKA condition. It may be that this band would be the degradation product of the protein. Since this lower band is only seen in the epitope-tagged Nato3 with PKA conditions (Figures 10 and 11), it may be that PKA action on Nato3 is promoting proteolytic cleavage. In this model, once the kinase acts on the protein, it then becomes a more suitable substrate for proteolytic cleavage giving a product that is lower in molecular weight after being cleaved, giving us the lower band that is observed on both of our SDS Page gel and Phos-tag gel (*Overview of Post-Translational Modification—US*, n.d.). Indeed PKA regulation of proteolysis has been demonstrated in developmental related proteins such as cubitus interruptus which acts as a regulator of Shh (Price & Kalderon, 1999).

This potentially observed cleavage product could be similar to the cleavage product observed with cubitus interruptus. Similar to what was observed with cubitus interruptus, it may be that the protein fragment has unique biological activity compared to the full length counterpart protein. When we modify Nato3 by PKA it could be that the cleavage event is important for inducting transcriptional activation for Nato3 or it may be that the cleavage product acts as a repressor. If a residue that acts as a phosphorylation site for Nato3 was substituted with an alanine amino acid, then we could test to see if the lower band associated with a cleavage product were to disappear. Future studies could then examine the nature and functionality of this fragment by expressing it in dopaminergic cells.

Potential phosphorylation sites for PKA

In cases of phosphorylation dependent mobility shift in SDS-PAGE, there is typically a robust change from one molecular weight to another. In the case of our Phos-Tag SDS PAGE we observe a smearing pattern. This may be due phosphorylation of Nato3 by PKA at multiple sites on the protein. We ran a kinase substrate motif recognition program that allowed us to predict which kinases were most likely to phosphorylate Nato3 at putative sites of phosphorylation. Serine 140 was of the sites that showed strong consensus with multiple algorithms (KinasePhos, NetPhos, NetPhosK, DISPHOS, Scansite3.0, and GPS3.0) for potential phosphorylation by PKA. This site is conserved among many bHLHs (Figure 13), and has been shown to be phosphorylated in the other bHLH proteins.

Serine 140 is highly predicted to be a substrate for PKA based on the kinase's known substrate consensus sequence, although a number of other residues could also be phosphorylated by PKA including those listed in Table 1. A search on the QPhos database showed that there is a phospho-peptide detected in HELA cells associated with the phosphorylated human Nato3 homolog to Serine 140 in mouse Nato3 (*QPhos: Quantitative Phosphoproteome for Heath-Related Studies*, n.d.). Indeed, the high stoichiometry of enzyme to substrate may cause residues with less substrate specificity to become phosphorylated in the overexpression conditions we tested in these cells. This could account for the smearing pattern that is observed in Figure 11 in the Nato3 with PKA condition. These sites could all be phosphorylated by PKA, giving the multiple levels of phosphorylation. For Nato3 Serine 140, Threonine 101 and Serine 89 are putative PKA

sites on Nato3 (see table 1). These sites could be residues that are phosphorylated with Serine 140 having the highest probability of phosphorylation based on the consensus sequence of PKA substrate.

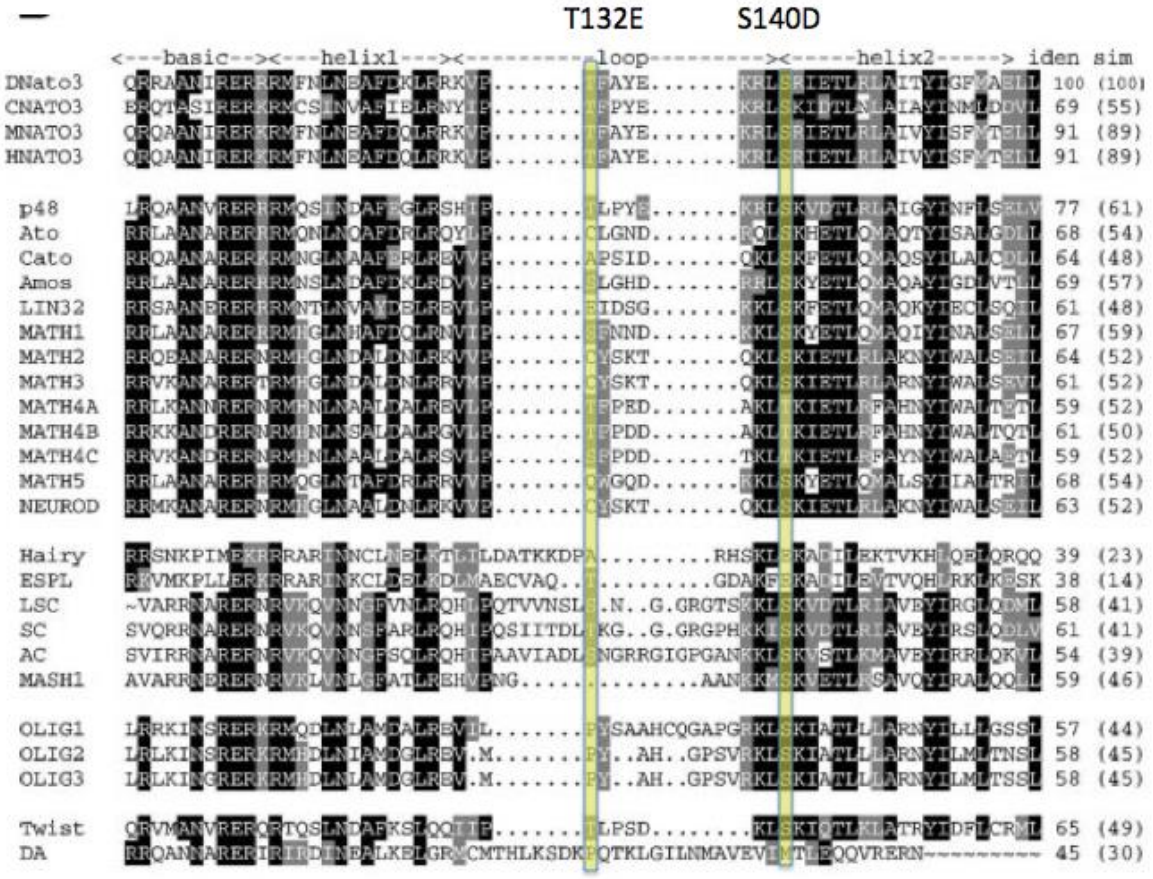

Figure 13: Potential phosphorylation sites on Nato3 are conserved among other bHLH proteins.

Mouse Nato3 ("MNATO3") amino acid residues of T132 and S140 align with residues conserved in many bHLH proteins (position of residue is highlighted by yellow box and mutations made at these residues are indicated). These residues are also conserved in the human Nato3 protein ("HNATO3"). S140 aligns with the residues that affect the function in the proneural protein MASH1 and the protein OLIG2 that drives the cell fate of neural progenitors into oligodendrocytes or motor neurons in the developing neural tube. Alignment from (Segev et al., 2001)

Tool	KinasePhos	NetPhos	NetPhosK	DISPHOS	Scansite3.0	GPS3.0
S89	-	-	-	+	+	+
T101	-	-	+	-	+	+
S140	+	+	+	+	+	+

Table 1: Common sites between phosphorylation prediction tools (Mouse Nato3)

We sent the Nato3 sequence to these prediction tools (KinasePhos, NetPhos, NetPhosK, DISPHOS, Scansite3.0 and GPS3.0) for the predicted phosphorylation sites. What is shown is the putative serine and threonine sites for the cyclic AMP dependent kinase PKA. Modified from (Segev et al., 2001).

Alternative explanations for results

An alternative explanation for our findings could be that the high expression of Nato3 protein as well as enzyme causes the phosphorylation of low affinity sites that are not physiologically relevant. Michaelis-Menten kinetics to estimate the substrate efficiency for an enzyme presumes a vanishingly small amount of enzyme relative to an abundant concentration of substrate to determine the substrate specificity for an enzyme (Roskoski, 2015). This is the basis of the algorithms that determine the optimal substrate for PKA, which is a dibasic sequence followed by a non-proline amino acid and then a serine or threonine (Xue et al., 2008). However at higher concentrations of enzyme, such as when we overexpress PKA in HEK cells along with the substrate, residues that are not as likely to be phosphorylated could become the target of the kinase simply by increasing the probability of enzyme-substrate interaction. This would make it possible for PKA to phosphorylate Nato3 when it would not be a substrate for PKA in physiological conditions. Indeed, there are other serine and threonine residues (T132, T144, S161) that could be

phosphorylated under non-physiological conditions. High concentrations of kinase and substrate may allow phosphorylation at these low-affinity binding sites.

To test this, putative serine or threonine residues could be analyzed for phosphorylation using in vitro kinase assay to determine the enzyme kinetics. This would entail identifying all of the serine and threonine residues that are phosphorylated by PKA using mass spectroscopy on the sample. We could replace all the potential phosphorylation sites (serine or threonine, such as the serine at position 140) with the amino acid alanine except the serine or threonine of interest to see if phosphorylation occurs. An alanine amino acid would not allow for a phosphorylation event to occur because the essential hydroxyl group found in serine is now just a hydrogen atom and this does not allow phosphate to bind to it. We could then determine the relative efficacy of PKA on those residues. However, just because there is a low substrate affinity for an enzyme does not mean it isn't physiologically relevant. Thus the most meaningful experiments to conduct are described in the sections entitled Physiological Implications and Future Studies.

Future Studies and physiological implications of Nato3 phosphorylation by PKA

Now that my part of the project has been completed the next step from those in the lab is to determine if Nato3 is phosphorylated by PKA using pure Nato3 protein. Isolating Nato3 from the rest of the cell proteins may yield insight into the phosphorylation status of Nato3 in the presence of PKA. The purified Nato3 will be obtained through immunoprecipitation using an antibody linked to magnetic beads (ThermoFisher) against the Flag epitope of the Nato3 protein. The isolated Nato3

protein can then be fractionated by SDS-PAGE and transferred to nitrocellulose for western blotting. Next, they could probe the nitrocellulose with antibodies against phospho-serine and phospho-threonine. Even if a mobility shift is not as visible as it was in our gels, then the probe against these phosphorylated proteins will help identify if the Nato3 in the presence of PKA is phosphorylated at those residues. Thus if our hypothesis is correct we will be able to identify antibody/western detection for phospho-serine and phospho-threonine in Nato3 when it is co-expressed with PKA, indicating that PKA is phosphorylating Nato3 at a threonine or serine site or potentially both.

In continuation of this project, the lab will also be determining the site of phosphorylation using mass spectrometry. Our lab has developed an in vivo screening approach to identify modifications of the Nato3 protein (Threonine 101, Threonine 132 and Serine 140) that can drive DA neuron genes important for dopamine neurogenesis including Nurr1. If we can show that Nato3 is phosphorylated by PKA at these serine or threonine residues this would give insight into the mechanism of action for Nato3 driving DA neurogenic genes. Mass spectrometry analysis will help us determine which residues are phosphorylated by using the peak intensities associated with Nato3 allowing us to determine where Nato3 is specifically phosphorylated. This will be done using purified Nato3 through the use of immunoprecipitation.

Through mass spectrometry we will be able to map and analyze phosphorylation sites with just ≥10 pmol of protein. This will give us a list of identified phosphorylation sites that matches a peptide containing site for peptide identification and the localization of the site (Dephoure, Gould, Gygi, & Kellogg, 2013).

Given what we have observed (Figures 8 and 9) the epitope-tagged Nato3 protein may be phosphorylated when in the presence of PKA. This could mean that phosphomimetic-Nato3 protein observed in the lab by other workers, (data not shown) may reflect that PKA can phosphorylate Nato3 during dopamine neurogenesis in vivo. However, there are some limitations to these observations. The HEK 293T cell line we used is a mammalian cell line not midbrain cells. This cell line is distinct due to the immortalization of the cells, the highly controlled environment of the continuous 5% CO2, 37°C, and ample nutrients being replenished every 3-4 days. This controlled environment is very different from the environment that would be present within in vivo conditions. We were able to overexpress both Nato3 and PKA in a cell line, therefore, this would not be the same as the physiological concentration expressed for an enzyme and substrate reaction in vivo, as described above.

In order to test to see if Nato3 is phosphorylated during dopamine neurogenesis, we would first need a Nato3 target-specific antibody with a high affinity for Nato3 that would allow us to detect the Nato3 protein endogenously. Future studies for in vivo testing could include the use of a mouse or chicken embryo. Using dopamine progenitor cells, collected at different stages of development using fluorescence-activated cell sorting (FACS) for cells that express the cell surface floor plate marker Corin, which has been successfully completed by Chung et al., 2009. After sorting the cells could be then plated onto a glass chamber (Ono et al., 2007) or lysis buffer and immunoprecipitation could be used against the endogenous Nato3 protein. The immuno-purified Nato3 protein would then be submitted for mass spectroscopic analysis to determine what residues are phosphorylated for Nato3 from an in vivo environment.

In order to determine the specific kinase that phosphorylates Nato3 in vivo, we would examine specific regions of the brain for the phosphorylated form of Nato using a phospho-specific antibody against phosphoserine 140 of Nato3 over the course of development. Specifically, comparing the expression of phosphorylated Nato3 over the course of dopamine neurogenesis. However, the limitation of this is that we do not know if serine140 is the key residue in this action. Our work currently underway (described in Future studies) would identify potential sites of action for PKA. If we are able to determine the specific residues, then we can mutate the residue(s) that are important like serine 140 to alanine in developing embryos and see if DA neurogenesis slows or even potentially stops altogether.

One more clinically relevant direction we would like to go in is to use mouse ESC with altered genomic DNA, like what has been done in (Li et al., 2011). Our goal is to identify the sites of phosphorylation by mass spectroscopy and then substitute the residue(s) with an alanine and see if this alters the amount of DA neuron generation. If so, we would then singularly add in the original amino acid, and see if we can then observe a greater generation of DA neurons in the mouse ESC. This could then give physiological relevance to not only the phosphorylation of Nato3, but the significance to the phosphorylated residue.

References

Alvarez-Fischer, D., Fuchs, J., Castagner, F., Stettler, O., Massiani-Beaudoin, O., Moya, K. L., Bouillot, C., Oertel, W. H., Lombès, A., Faigle, W., Joshi, R. L., Hartmann, A., & Prochiantz, A. (2011). Engrailed protects mouse midbrain dopaminergic neurons against mitochondrial complex I insults. *Nature Neuroscience*, *14*(10), 1260–1266. https://doi.org/10.1038/nn.2916

Andersson, E., Jensen, J. B., Parmar, M., Guillemot, F., & Björklund, A. (2006). Development of the mesencephalic dopaminergic neuron system is compromised in the absence of neurogenin 2. *Development*, *133*(3), 507–516. https://doi.org/10.1242/dev.02224

Ang, S.-L. (2006). Transcriptional control of midbrain dopaminergic neuron development. *Development*, *133*(18), 3499–3506. https://doi.org/10.1242/dev.02501

Balagurumoorthy, P., Adelstein, S. J., & Kassis, A. I. (2008). Method to eliminate linear DNA from mixture containing nicked circular, supercoiled, and linear plasmid DNA. *Analytical Biochemistry*, *381*(1), 172–174. https://doi.org/10.1016/j.ab.2008.06.037

Benskey, M. J., Perez, R. G., & Manfredsson, F. P. (2016). The contribution of alpha synuclein to neuronal survival and function – Implications for Parkinson's disease. *Journal of Neurochemistry*, *137*(3), 331–359. https://doi.org/10.1111/jnc.13570

Bertrand, N., Castro, D. S., & Guillemot, F. (2002). Proneural genes and the specification of neural cell types. *Nature Reviews Neuroscience*, *3*(7), 517–530. https://doi.org/10.1038/nrn874

Braak, H., Tredici, K. D., Rüb, U., de Vos, R. A. I., Jansen Steur, E. N. H., & Braak, E. (2003). Staging of brain pathology related to sporadic Parkinson's disease. *Neurobiology of Aging*, *24*(2), 197–211. https://doi.org/10.1016/S0197-4580(02)00065-9

Chung, S., Leung, A., Han, B.-S., Chang, M.-Y., Moon, J.-I., Kim, C.-H., Hong, S., Pruszak, J., Isacson, O., & Kim, K.-S. (2009). Wnt1-lmx1a Forms a Novel Autoregulatory Loop and Controls Midbrain Dopaminergic Differentiation Synergistically with the SHH-FoxA2

Pathway. *Cell Stem Cell*, *5*(6), 646–658. https://doi.org/10.1016/j.stem.2009.09.015

Corp, S. A. (n.d.). *Cloning and Expression—FLAG and 3xFLAG Overview*. 2.

Dauer, W., & Przedborski, S. (2003). Parkinson's Disease: Mechanisms and Models. *Neuron*, *39*(6), 889–909. https://doi.org/10.1016/S0896-6273(03)00568-3

Dawson, T. M., & Dawson, V. L. (2003). Molecular pathways of neurodegeneration in Parkinson's disease. *Science; Washington*, *302*(5646), 819–822.

Doucet-Beaupré, H., Gilbert, C., Profes, M. S., Chabrat, A., Pacelli, C., Giguère, N., Rioux, V., Charest, J., Deng, Q., Laguna, A., Ericson, J., Perlmann, T., Ang, S.-L., Cicchetti, F., Parent, M., Trudeau, L.-E., & Lévesque, M. (2016). Lmx1a and Lmx1b regulate mitochondrial functions and survival of adult midbrain dopaminergic neurons. *Proceedings of the National Academy of Sciences*, *113*(30), E4387–E4396. https://doi.org/10.1073/pnas.1520387113

Ellis, C. E., Murphy, E. J., Mitchell, D. C., Golovko, M. Y., Scaglia, F., Barceló-Coblijn, G. C., & Nussbaum, R. L. (2005). Mitochondrial Lipid Abnormality and Electron Transport Chain Impairment in Mice Lacking α-Synuclein. *Molecular and Cellular Biology*, *25*(22), 10190–10201. https://doi.org/10.1128/MCB.25.22.10190-10201.2005

Hyland, K., & Clayton, P. T. (1992). Aromatic L-amino acid decarboxylase deficiency: Diagnostic methodology. *Clinical Chemistry*, *38*(12), 2405–2410.

Kalia, L. V., & Lang, A. E. (2015). Parkinson's disease. *The Lancet; London*, *386*(9996), 896–912. http://dx.doi.org/10.1016/S0140-6736(14)61393-3

Keller, M. J., Wu, A. W., Andrews, J. I., McGonagill, P. W., Tibesar, E. E., & Meier, J. L. (2007). Reversal of Human Cytomegalovirus Major Immediate-Early Enhancer/Promoter Silencing in Quiescently Infected Cells via the Cyclic AMP Signaling Pathway. *Journal of Virology*, *81*(12), 6669–6681. https://doi.org/10.1128/JVI.01524-06

Kinoshita, E., Kinoshita-kikuta, E., & Koike, T. (2009). Separation and detection of large phosphoproteins using Phos-tag SDS-PAGE. *Nature Protocols; London*, *4*(10), 1513–

1521. http://dx.doi.org.ezproxy.gvsu.edu/10.1038/nprot.2009.154

Konsoula, Z. (2020). Myc Antibody Review. *Materials and Methods*. /method/Myc-Antibody-Review.html

LeWitt, P. A. (2015). Levodopa therapy for Parkinson's disease: Pharmacokinetics and pharmacodynamics. *Movement Disorders*, *30*(1), 64–72. https://doi.org/10.1002/mds.26082

Li, H., Paes de Faria, J., Andrew, P., Nitarska, J., & Richardson, W. D. (2011). Phosphorylation Regulates OLIG2 Cofactor Choice and the Motor Neuron-Oligodendrocyte Fate Switch. *Neuron*, *69*(5), 918–929. https://doi.org/10.1016/j.neuron.2011.01.030

Ma, Y., Tang, C., Chaly, T., Greene, P., Breeze, R., Fahn, S., Freed, C., Dhawan, V., & Eidelberg, D. (2010). Dopamine Cell Implantation in Parkinson's Disease: Long-Term Clinical and 18F-FDOPA PET Outcomes. *Journal of Nuclear Medicine*, *51*(1), 7–15. https://doi.org/10.2967/jnumed.109.066811

Mansour, A. A., Nissim-Eliraz, E., Zisman, S., Golan-Lev, T., Schatz, O., Klar, A., & Ben-Arie, N. (n.d.). *Is Nato3 a Novel Regulator of Floor Plate and Spinal Cord Development?* 1.

Massari, M. E., & Murre, C. (2000). Helix-Loop-Helix Proteins: Regulators of Transcription in Eucaryotic Organisms. *Molecular and Cellular Biology*, *20*(2), 429–440.

Miller, F. D., & Gauthier, A. S. (2007). Timing Is Everything: Making Neurons versus Glia in the Developing Cortex. *Neuron*, *54*(3), 357–369. https://doi.org/10.1016/j.neuron.2007.04.019

Morizane, A., Li, J.-Y., & Brundin, P. (2008). From bench to bed: The potential of stem cells for the treatment of Parkinson's disease. *Cell and Tissue Research; Heidelberg*, *331*(1), 323–336. http://dx.doi.org/10.1007/s00441-007-0541-0

Niu, W., Zang, T., Wang, L.-L., Zou, Y., & Zhang, C.-L. (2018). Phenotypic Reprogramming of Striatal Neurons into Dopaminergic Neuron-like Cells in the Adult Mouse Brain. *Stem Cell Reports*, *11*(5), 1156–1170. https://doi.org/10.1016/j.stemcr.2018.09.004

Nouri, N., & Awatramani, R. (2017). A novel floor plate boundary defined by adjacent En1 and Dbx1 microdomains distinguishes midbrain dopamine and hypothalamic neurons. *Development*, *144*(5), 916–927. https://doi.org/10.1242/dev.144949

Nunes, I., Tovmasian, L. T., Silva, R. M., Burke, R. E., & Goff, S. P. (2003). Pitx3 is required for development of substantia nigra dopaminergic neurons. *Proceedings of the National Academy of Sciences of the United States of America*, *100*(7), 4245–4250. https://doi.org/10.1073/pnas.0230529100

Omodei, D., Acampora, D., Mancuso, P., Prakash, N., Di Giovannantonio, L. G., Wurst, W., & Simeone, A. (2008). Anterior-posterior graded response to Otx2 controls proliferation and differentiation of dopaminergic progenitors in the ventral mesencephalon. *Development*, *135*(20), 3459–3470. https://doi.org/10.1242/dev.027003

Ono, Y., Nakatani, T., Minaki, Y., & Kumai, M. (2010). The basic helix-loop-helix transcription factor Nato3 controls neurogenic activity in mesencephalic floor plate cells. *Development*, *137*(11), 1897–1906. https://doi.org/10.1242/dev.042572

Ono, Y., Nakatani, T., Sakamoto, Y., Mizuhara, E., Minaki, Y., Kumai, M., Hamaguchi, A., Nishimura, M., Inoue, Y., Hayashi, H., Takahashi, J., & Imai, T. (2007). Differences in neurogenic potential in floor plate cells along an anteroposterior location: Midbrain dopaminergic neurons originate from mesencephalic floor plate cells. *Development*, *134*(17), 3213–3225. https://doi.org/10.1242/dev.02879

Palmer, C., Coronel, R., Bernabeu-Zornoza, A., & Liste, I. (2019). Therapeutic Application of Stem Cell and Gene Therapy in Parkinson's Disease. In S. Singh & N. Joshi (Eds.), *Pathology, Prevention and Therapeutics of Neurodegenerative Disease* (pp. 159–171). Springer Singapore. https://doi.org/10.1007/978-981-13-0944-1_14

Parmar, M., Grealish, S., & Henchcliffe, C. (2020). The future of stem cell therapies for Parkinson disease. *Nature Reviews. Neuroscience*, *21*(2), 103–115. https://doi.org/10.1038/s41583-019-0257-7

Parmar, M., Torper, O., & Drouin-Ouellet, J. (2019). Cell-based therapy for Parkinson's disease: A journey through decades toward the light side of the Force. *European Journal of Neuroscience*, *49*(4), 463–471. https://doi.org/10.1111/ejn.14109

Parras, C. M., Schuurmans, C., Scardigli, R., Kim, J., Anderson, D. J., & Guillemot, F. (2002). Divergent functions of the proneural genes Mash1 and Ngn2 in the specification of neuronal subtype identity. *Genes & Development*, *16*(3), 324–338. https://doi.org/10.1101/gad.940902

Perez, S. E., Rebelo, S., & Anderson, D. J. (1999). Early specification of sensory neuron fate revealed by expression and function of neurogenins in the chick embryo. *Development (Cambridge, England)*, *126*(8), 1715–1728.

Peterson, D. J., Marckini, D. N., Straight, J. L., King, E. M., Johnson, W., Sarah, S. S., Chowdhary, P. K., & DeLano-Taylor, M. K. (2019). The Basic Helix-Loop-Helix Gene Nato3 Drives Expression of Dopaminergic Neuron Transcription Factors in Neural Progenitors. *Neuroscience*, *421*, 176–191. https://doi.org/10.1016/j.neuroscience.2019.09.003

Price, M. A., & Kalderon, D. (1999). Proteolysis of cubitus interruptus in Drosophila requires phosphorylation by protein kinase A. *Development*, *126*(19), 4331–4339.

qPhos: Quantitative phosphoproteome for heath-related studies. (n.d.). Retrieved May 19, 2020, from http://qphos.cancerbio.info/show.php?type=simple

Raposo, A. A. S. F., Vasconcelos, F. F., Drechsel, D., Marie, C., Johnston, C., Dolle, D., Bithell, A., Gillotin, S., van den Berg, D. L. C., Ettwiller, L., Flicek, P., Crawford, G. E., Parras, C. M., Berninger, B., Buckley, N. J., Guillemot, F., & Castro, D. S. (2015). Ascl1 Coordinately Regulates Gene Expression and the Chromatin Landscape during Neurogenesis. *Cell Reports*, *10*(9), 1544–1556. https://doi.org/10.1016/j.celrep.2015.02.025

Rath, A., Glibowicka, M., Nadeau, V. G., Chen, G., & Deber, C. M. (2009). Detergent binding

explains anomalous SDS-PAGE migration of membrane proteins. *Proceedings of the National Academy of Sciences*, *106*(6), 1760–1765. https://doi.org/10.1073/pnas.0813167106

Reynolds, J. A., & Tanford, C. (1970). Binding of Dodecyl Sulfate to Proteins at High Binding Ratios. Possible Implications for the State of Proteins in Biological Membranes. *Proceedings of the National Academy of Sciences of the United States of America*, *66*(3), 1002–1007. JSTOR.

Roskoski, R. (2015). Michaelis-Menten Kinetics☆. In *Reference Module in Biomedical Sciences*. Elsevier. https://doi.org/10.1016/B978-0-12-801238-3.05143-6

Sambrook, J., & Russell, D. W. (2006). Directional Cloning into Plasmid Vectors. *Cold Spring Harbor Protocols*, *2006*(1), pdb.prot3919. https://doi.org/10.1101/pdb.prot3919

Schapira, A. H. (2008). Mitochondria in the aetiology and pathogenesis of Parkinson's disease. *The Lancet Neurology*, *7*(1), 97–109. https://doi.org/10.1016/S1474-4422(07)70327-7

Segev, E., Halachmi, N., Salzberg, A., & Ben-Arie, N. (2001). Nato3 is an evolutionarily conserved bHLH transcription factor expressed in the CNS of Drosophila and mouse. *Mechanisms of Development*, *106*(1–2), 197–202. https://doi.org/10.1016/S0925-4773(01)00437-3

Shirahama, K., Tsujii, K., & Takagi, T. (1974). Free-boundary electrophoresis of sodium dodecyl sulfate-protein polypeptide complexes with special reference to SDS-polyacrylamide gel electrophoresis. *Journal of Biochemistry*, *75*(2), 309–319. https://doi.org/10.1093/oxfordjournals.jbchem.a130398

Smith, Y., Bennett, B. D., Bolam, J. P., Parent, A., & Sadikot, A. F. (1994). Synaptic relationships between dopaminergic afferents and cortical or thalamic input in the sensorimotor territory of the striatum in monkey. *Journal of Comparative Neurology*, *344*(1), 1–19. https://doi.org/10.1002/cne.903440102

Sveinbjornsdottir, S. (2016). The clinical symptoms of Parkinson's disease. *Journal of Neurochemistry*, *139*(S1), 318–324. https://doi.org/10.1111/jnc.13691

Van Den Eeden, S. K. (2003). Incidence of Parkinson's Disease: Variation by Age, Gender, and Race/Ethnicity. *American Journal of Epidemiology*, *157*(>11), 1015–1022. https://doi.org/10.1093/aje/kwg068

Viñals, F., Reiriz, J., Ambrosio, S., Bartrons, R., Rosa, J. L., & Ventura, F. (2004). BMP-2 decreases Mash1 stability by increasing Id1 expression. *The EMBO Journal*, *23*(17), 3527–3537. https://doi.org/10.1038/sj.emboj.7600360

Vossius, C., Nilsen, O. B., & Larsen, J. P. (2009). Parkinson's disease and nursing home placement: The economic impact of the need for care. *European Journal of Neurology*, *16*(2), 194–200. https://doi.org/10.1111/j.1468-1331.2008.02380.x

Xue, Y., Ren, J., Gao, X., Jin, C., Wen, L., & Yao, X. (2008). GPS 2.0, a Tool to Predict Kinase-specific Phosphorylation Sites in Hierarchy. *Molecular & Cellular Proteomics*, *7*(9), 1598–1608. https://doi.org/10.1074/mcp.M700574-MCP200